DEPARTMENT OF MECHANICAL ENGINEERING AND MECHANICS
COLLEGE OF ENGINEERING AND TECHNOLOGY
OLD DOMINION UNIVERSITY
NORFOLK, VIRGINIA 23508

COMPONENT MODE SYNTHESIS AND LARGE DEFLECTION VIBRATION OF COMPLEX STRUCTURES

VOLUME 2: SINGLE-MODE LARGE DEFLECTION VIBRATIONS OF BEAMS AND PLATES USING FINITE ELEMENT METHOD

By

Chuh Mei, Principal Investigator

and

Mo-How Shen

Final Report
For the period ended January 31, 1987

Prepared for the
National Aeronautics and Space Administration
Langley Research Center
Hampton, VA 23665

Under
Research Grant NAG-1-301
Mr. Joseph E. Walz, Technical Monitor
SDD-Structural Dynamics Branch

August 1987

DEPARTMENT OF MECHANICAL ENGINEERING AND MECHANICS
COLLEGE OF ENGINEERING AND TECHNOLOGY
OLD DOMINION UNIVERSITY
NORFOLK, VIRGINIA 23508

COMPONENT MODE SYNTHESIS AND LARGE DEFLECTION VIBRATION OF COMPLEX STRUCTURES

VOLUME 2: SINGLE-MODE LARGE DEFLECTION VIBRATIONS OF BEAMS AND PLATES USING FINITE ELEMENT METHOD

By

Chuh Mei, Principal Investigator

and

Mo-How Shen

Final Report
For the period ended January 31, 1987

Prepared for the
National Aeronautics and Space Administration
Langley Research Center
Hampton, VA 23665

Under
Research Grant NAG-1-301
Mr. Joseph E. Walz, Technical Monitor
SDD-Structural Dynamics Branch

Submitted by the
Old Dominion University Research Foundation
P.O. Box 6369
Norfolk, Virginia 23508

August 1987

TABLE OF CONTENTS

LIST OF TABLES

TABLE OF CONTENTS - Continued

LIST OF TABLES - Concluded

LIST OF FIGURES

LIST OF FIGURES - Concluded

FINITE ELEMENT ANALYSIS OF NONLINEAR FORCED VIBRATIONS OF BEAMS AND RECTANGULAR PLATES

Chuh Mei* and Kamolphan Decha-Umphait†
Old Dominion University, Norfolk, Virginia

SUMMARY

Slender beams and thin plate structures subjected to periodic loading are likely to encounter oscillations large in comparison to beam depth or plate thickness. The responses predicted using the small deflection linear structure theory are, therefore, no longer applicable. Nonlinear theory, taking into account the effects of large amplitude, must be employed.

In this report, a finite element method is presented for the large amplitude vibrations of complex structures which can be modelled with beam and rectangular plate elements subjected to harmonic excitation. Both in-plane deformation and inertia are considered in the formulation. The method described would give more accurate results than the classic continuum approaches which neglect the effects of inplane inertia. Derivation of the harmonic force and nonlinear stiffness matrices for a beam and a rectangular plate element are presented. Solution procedures and convergence characteristics of the finite element method are described. Nonlinear response to uniform and concentrated harmonic loadings, and improved nonlinear free vibration results are presented for beams and rectangular plates of various boundary conditions.

---

*Associate Professor, Mechanical Engineering and Mechanics
†Graduate Student

INTRODUCTION

Linear models have had, and will continue to have, great importance in the analysis of real structural systems. There are, however, some dynamic systems which are inherently nonlinear and their behavior cannot be described fully through linear models alone.

NASA is considering placing in orbit various large, flexible, and low density space structures. These structures, or some components of these structures, may be expected to have oscillations large in comparison to some corresponding dimension (beam depth or plate thickness). In this situation, the responses predicted using the small deflection linear structure theory may no longer be valid, therefore, nonlinear structure theory taking account the effects of large deflection may have to be employed.

The first papers that dealt with nonlinear vibrations of beams and plates with immovable edge supports were those of Woinowsky-Krieger (ref. 1) and Herrmann (refs. 2 and 3). Herrmann presented a set of equations of motions that corresponds to the dynamic analogue of the von Karman plate theory. The nonlinear beam vibration was treated as a special case of plate vibration in reference 3. Although the basic equations had been thus established, the general solutions of the coupled, nonlinear, governing differential equations of motion are still not available owing to the mathematical difficulties involved. The classical continuum approach was to employ various approximate methods to beams and plates of simple geometrical shape and of simple restraint conditions along the edges.

Nonlinear forced vibration of beams with different boundary conditions has been investigated by applying the Galerkin method (e.g. refs. 4 to 7) and the resulting equations were solved by the harmonic balance method. Other approaches to the problem, namely the finite element method combined

with method of averaging, the form-function approximation method and the incremental time-space finite strip method were proposed by Busby and Weingarten (ref. 8), Lou and Sikarskie (ref. 9) and Cheung and Lau (ref. 10), respectively. Further, a perturbation procedure based on the method of multiple time scales has been presented by Nayfeh et al. (refs. 11 and 12). Eisley (ref. 13) and Sathyamoorthy (ref. 14) have presented their comprehensive and excellent reviews on nonlinear analyses of beams concerning the classical methods.

Nonlinear forced vibrations of circular and rectangular plates with various boundary conditions have also been investigated by using the Galerkin or Ritz method (refs. 4, 5 and 15 to 18), the Kantorovich averaging method (refs. 19 and 20), various perturbation methods (ref. 21 to 24), and incremental harmonic balance method (ref. 25). Studies based on the simplified Berger's hypothesis (ref. 26) have also been made with the use of the Galerkin method (refs. 27 and 28). Yamaki et al. (ref. 18), Chia (ref. 29) and Sythamoorthy (ref. 30) have presented their comprehensive reviews on both free and forced nonlinear vibrations of plates.

The finite element method has proven to be an extremely powerful tool for complex structures. Applications of the finite element method to large amplitude free vibrations of beams and rectangular plates was first presented by Mei (refs. 31 and 32). The inplane tensile force induced by the transverse deflection alone was assumed to be constant for each individual beam or plate element. Nonlinear frequencies of beams and rectangular plates with various boundary conditions agreed well with the approximate continuum solutions of Woinowsky-Krieger (ref. 1), Chu and Herrmann (ref. 3), Yamaki (ref. 15) and Evensen (ref. 33). Rao et al. proposed a novel scheme of linearizing the nonlinear strain-displacement relations in formu-

lating the nonlinear stiffness matrix. They studied nonlinear free vibrations of beams and circular plates (ref. 34) and rectangular plates (refs. 35 and 36). Shear deformation and rotary inertia were also included in the formulation (refs. 37 and 38). Reddy and Stricklin (ref. 39) presented a linear and a quadratic isoparametric rectangular element using the linearized Reissner-type variational formulation to study large amplitude free plate vibrations. Inplane displacements were considered in their formulation. Two triangular elements have also been developed for nonlinear free vibrations of plates of arbitrary shape. The first one (ref. 40) is consistent with the higher-order bending element TRPLT1 (ref. 41) in NASTRAN®, and the second one (ref. 42) is consistent with the high-precision plate element of Cowper et al. (ref. 43). The solutions obtained for numerical examples include rectangular, circular, rhombic and isosceles triangular plates. Reddy and Chao (refs. 44 and 45) extended the earlier isoparametric rectangular elements to include transverse shear and laminated composite materials. Mei et al. (46) also extended the earlier triangular element to include laminated composite materials.

Bhashyan and Prathap (ref. 47) and Sarma and Varadan (refs. 48 and 49) also presented a Galerkin and a Lagrange-type finite element formulation for nonlinear free vibrations of beams with ends restrained from longitudinal movement. They obtained frequency values at the instant of maximum amplitude which was based on a new criterion for defining nonlinear frequency presented in references 50 and 51. However, the results (refs. 47 to 50) do not agree with those classic continuum solutions (refs. 1 and 33). What they actually solved is a linear beam vibration problem subjected to an initial axial tensile force as commented on in reference 52.

In this report, a finite element formulation is presented for large

amplitude vibrations of slender beams and thin plates subjected to harmonic excitation. Harmonic force matrices are developed for nonlinear vibrations of a beam and a rectangular plate element under uniform harmonic loading. Longitudinal or inplane deformation and inertia are both included in the formulation. These effects were neglected in the earlier finite element nonlinear free vibration analyses (refs. 31, 32, 34 to 38, 40, 42 and 46). Formulation of the harmonic force matrix [p] is based on the first order approximation of solutions of a Duffing system given by Hsu (ref. 53). He showed that the simple harmonic forcing function $P_0 \cos\omega\tau$ is the first order approximation of the elliptic forcing function $BAcn(\lambda\tau,n)$, and the well-known perturbation solution of a Duffing system to a simple harmonic forcing function is the first order approximation of the simple elliptic response $Acn(\lambda\tau,n)$. Derivation of the harmonic force and nonlinear stiffness matrices are given. Nonlinear forced response to uniform and simulated concentrated (uniform load on short beam segment) harmonic loadings, and improved nonlinear free vibration results are presented for beams and rectangular plates with various boundary conditions. Finite element results are compared with approximate solutions of elliptic function response, perturbation method and other numerical approaches.

SYMBOLS

A	amplitude = w_{max}/h for plate (w_{max}/R for beam)
B	nondimensional forcing amplitude factor
a, b	length and width of rectangular plate
$\bar{a}$, $\bar{b}$	length and width of rectangular plate element
[C]	extensional material stiffness matrix
c	constant defined in equations (46) and (47)
[D]	bending material stiffness matrix
d	length of the loaded element
E	Young's modulus
{e}	membrane strains
[F]	linearizing function matrix defined in equation (27)
f_1, f_2	linearizing functions
[G]	matrix relating generalized coordinates and membrane strains defined in equation (26)
[H]	matrix relating generalized coordinates and curvatures defined in equation (23)
h	thickness of plate
I	area moment of inertia of beam
[K]	system linear stiffness matrix
$[\bar{K}]$	system nonlinear stiffness matrix
[k]	element stiffness matrix
$[\bar{k}]$	element nonlinear stiffness matrix
L	length of beam
$\bar{L}$	mathematical operator defined in equations (34) and (35)
ℓ	length of a beam element
$\{M_o\}$	bending and twisting moments

$[M]$	system mass matrix
$[m]$	element consistent mass matrix
$\{N\}$	membrane resultant forces
$[P]$	system harmonic force matrix
P_o	nondimensional forcing parameter
$[p]$	element harmonic force matrix
$[Q]$	matrix relating generalized coordinates and linearizing function defined in equation (25)
R	radius of gyration of beam cross-section
S	beam cross-sectional area
$[T_b]$, $[T_m]$	matrix relating element nodal displacements and generalized coordinates defined in equations (21) and (22)
T	kinetic energy
t	time
U	strain energy
u, v, w	displacements
x, y, z	coordinates
α_i, β_i	generalized coordinates
β	nonlinear coefficient in Duffing equation
γ	shear strain
$\{\delta\}$	element nodal displacements
$\{\varepsilon\}$	strains
η	modulus of elliptic function
$\{\kappa\}$	curvatures
λ	circular frequency of elliptic function
ν	Poisson's ratio
ξ	norm
ρ	mass density
τ	nondimensional time

$\{\phi\}$	mode shape normalized to unit value of the largest component
ψ	stress function
ω	frequency

Subscripts:

b	bending
L	linear
m	membrane

FINITE ELEMENT FORMULATION

Strain and Kinetic Energies

From von Karman's large deflection plate theory, the nonlinear strain-displacement relations are defined as

$$\{\varepsilon\} = \{e\} + z\{\kappa\} \tag{1}$$

where the membrane or midsurface strains $\{e\}$ and curvatures $\{\kappa\}$ are given by

$$\{e\} = \begin{Bmatrix} \frac{\partial u}{\partial x} + \frac{1}{2}\left(\frac{\partial w}{\partial x}\right)^2 \\ \frac{\partial v}{\partial y} + \frac{1}{2}\left(\frac{\partial w}{\partial y}\right)^2 \\ \frac{\partial u}{\partial y} + \frac{\partial v}{\partial x} + \frac{\partial w}{\partial x}\frac{\partial w}{\partial y} \end{Bmatrix} \tag{2}$$

$$\{\kappa\} = \begin{Bmatrix} -\frac{\partial^2 w}{\partial x^2} \\ -\frac{\partial^2 w}{\partial y^2} \\ -2\frac{\partial^2 w}{\partial x \partial y} \end{Bmatrix} \tag{3}$$

and u, v, w are displacements of the plate midsurface in the x, y, z - directions, respectively.

The membrane or inplane resultant forces $\{N\}$ and bending and twisting moments $\{M_0\}$ are related to the strains and curvatures by

$$\{N\} = \begin{Bmatrix} N_x \\ N_y \\ N_{xy} \end{Bmatrix} = [C]\{e\} \tag{4}$$

$$\{M_o\} = \begin{Bmatrix} M_x \\ My \\ M_{xy} \end{Bmatrix} = [D]\{\kappa\} \tag{5}$$

where $[C]$ and $[D]$ are the extensional and bending material stiffness matrices, respectively. For plates of isotropic material and uniform thickness h, the material stiffness matrices are

$$[C] = \frac{Eh}{1-\nu^2} \begin{bmatrix} 1 & \nu & 0 \\ \nu & 1 & 0 \\ 0 & 0 & \frac{1-\nu}{2} \end{bmatrix} \tag{6}$$

$$[D] = \frac{Eh^3}{12(1-\nu^2)} \begin{bmatrix} 1 & \nu & 0 \\ \nu & 1 & 0 \\ 0 & 0 & \frac{1-\nu}{2} \end{bmatrix} \tag{7}$$

where E and ν are the Young's modulus and Poisson's ratio, respectively.

The total strain energy for a plate element is given by

$$U = U_b + U_m \tag{8}$$

with

$$U_b = \frac{1}{2} \iint \{M_o\}^T \{\kappa\} \, dx \, dy$$

$$= \frac{1}{2} \iint \{\kappa\}^T [D] \{\kappa\} \, dx \, dy \qquad (9)$$

$$U_m = \frac{1}{2} \iint \{N\}^T \{e\} \, dx \, dy$$

$$= \frac{1}{2} \iint \{e\}^T [C] \{e\} \, dx \, dy \qquad (10)$$

where the subscripts b and m denote the bending and membrane components, respectively.

The kinetic energy of a plate element executing harmonic oscillations is

$$T = \frac{1}{2} \rho h \iint (\dot{u}^2 + \dot{v}^2 + \dot{w}^2) \, dx \, dy \qquad (11)$$

where ρ is the mass density and $(\cdot)$ means differentiation with respect to time t.

Similar expressions for a beam element can be obtained from the corresponding plate equations (1) to (11) by letting

$$v = 0$$

$$\frac{\partial (\ )}{\partial y} = 0$$

$$[C] = ES$$

$$[D] = EI \tag{12}$$

where S and I are the area and moment of inertia of the beam cross-section, respectively. These beam equations are given in Appendix A.

Plate Element

The finite element used in the present formulation shown in figure 1 is the conforming rectangular plate with 24 degrees-of-freedom due to Bogner et al. (ref. 54). The displacement functions within the element are assumed as

$$\begin{aligned} w = {} & \alpha_1 + \alpha_2 x + \alpha_3 y + \alpha_4 x^2 + \alpha_5 xy + \alpha_6 y^2 \\ & + \alpha_7 x^3 + \alpha_8 x^2 y + a_9 xy^2 + \alpha_{10} y^3 \\ & + \alpha_{11} x^3 y + \alpha_{12} x^2 y^2 + \alpha_{13} xy^3 \\ & + \alpha_{14} x^3 y^2 + \alpha_{15} x^2 y^3 + \alpha_{16} x^3 y^3 \end{aligned} \tag{13}$$

$$u = \beta_1 + \beta_2 x + \beta_3 y + \beta_4 xy \tag{14}$$

$$v = \beta_5 + \beta_6 x + \beta_7 y + \beta_8 xy \tag{15}$$

The twenty four generalized coordinates

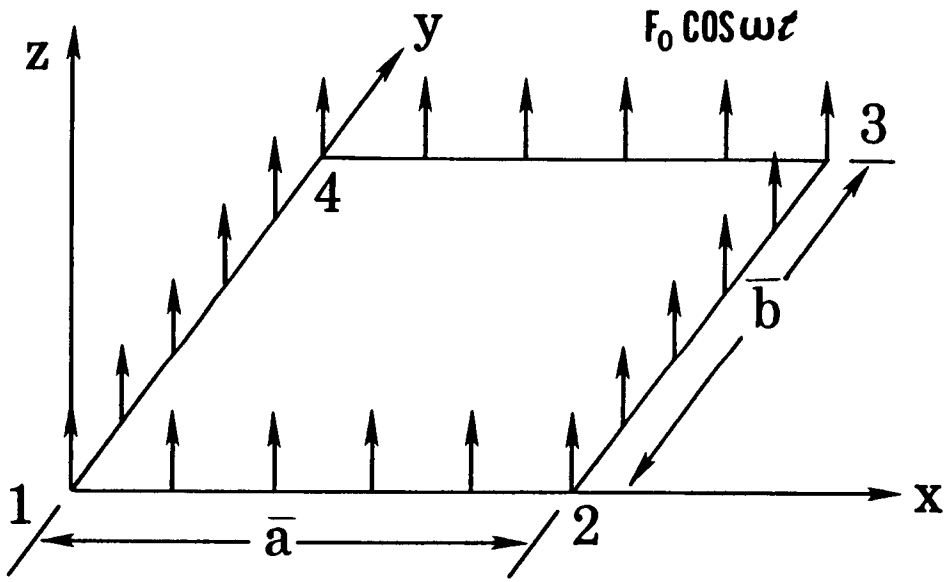

Figure 1. Rectangular plate element.

$$\{\alpha\}^T = [\alpha_1, \alpha_2, \ldots, \alpha_{16}] \tag{16}$$

$$\{\beta\}^T = [\beta_1, \beta_2, \ldots, \beta_8] \tag{17}$$

can be determined from the element nodal displacements

$$\{\delta\}^T = [\{\delta_b\}^T, \{\delta_m\}^T] \tag{18}$$

with

$$\{\delta_b\}^T = [W_1, W_2, W_3, W_4, W_{x1}, \ldots, W_{y1}, \ldots, W_{xy1}, \ldots, W_{xy4}] \tag{19}$$

$$\{\delta_m\}^T = [U_1, U_2, U_3, U_4, V_1, V_2, V_3, V_4] \tag{20}$$

The relationship between the generalized coordinates and the element nodal displacements can be written as

$$\{\alpha\} = [T_b]\{\delta_b\} \tag{21}$$

$$\{\beta\} = [T_m]\{\delta_m\} \tag{22}$$

Substituting equation (13) into equation (3), the curvatures can be expressed in terms of the generalized coordinates as

$$\{\kappa\} = [H]\{\alpha\} \tag{23}$$

The bending strain energy U_b of equation (9) leads to the element linear bending stiffness matrix

$$[k_b] = [T_b]^T \iint [H]^T[D][H]\, dx\, dy\, [T_b] \tag{24}$$

Similarly, the kinetic energy T of equation (11) leads to the element consistent mass matrices $[m_b]$ and $[m_m]$. These three matrices can be found explicitly in reference 54.

The membrane strain energy U_m of equation (10) can be linearized utilizing the linearizing functions

$$\{f\} = \begin{Bmatrix} f_1 \\ f_2 \end{Bmatrix} = \frac{1}{2} \begin{Bmatrix} \frac{\partial w}{\partial x} \\ \frac{\partial w}{\partial y} \end{Bmatrix} = \frac{1}{2}\,[Q]\{\alpha\}$$

$$= \frac{1}{2}\,[Q]\,[T_b]\{\delta_b\} \tag{25}$$

where the element displacements $\{\delta_b\}$ are obtained from the plate deflection through an iterative procedure discussed in the next section. Thus, the membrane strains of equation (2) become

$$\{e\} = [F] \begin{Bmatrix} \frac{\partial w}{\partial x} \\ \frac{\partial w}{\partial y} \end{Bmatrix} + \begin{Bmatrix} \frac{\partial u}{\partial x} \\ \frac{\partial v}{\partial y} \\ \frac{\partial u}{\partial y} + \frac{\partial v}{\partial x} \end{Bmatrix}$$

$$= [F][Q]\{\alpha\} + [G]\{\beta\}$$

$$= \left[[F][Q] \,\vdots\, [G] \right] \begin{Bmatrix} \{\alpha\} \\ \{\beta\} \end{Bmatrix} \tag{26}$$

with

$$[F] = \begin{bmatrix} f_1 & 0 \\ 0 & f_2 \\ f_2 & f_1 \end{bmatrix} \tag{27}$$

and the linearized membrane strain energy in terms of the element nodal displacements is

$$U_m = \frac{1}{2} \left[\{\delta_b\}^T \{\delta_m\}^T \right] \left[\begin{bmatrix} [\bar{k}_b] & [\bar{k}_{bm}] \\ [\bar{k}_{mb}] & 0 \end{bmatrix} + \begin{bmatrix} 0 & 0 \\ 0 & [k_m] \end{bmatrix} \right] \begin{Bmatrix} \{\delta_b\} \\ \{\delta_m\} \end{Bmatrix} \tag{28}$$

where the element linear membrane stiffness matrix is given by

$$[k_m] = [T_m]^T \iint [G]^T [C][G] dx\, dy [T_m] \tag{29}$$

This $[k_m]$ matrix is also given explicitly in reference 54. The submatrices of the linearized nonlinear stiffness matrix $[\bar{k}]$ are given by

$$[\bar{k}_b] = [T_b]^T \iint [Q]^T [F]^T [C] [F] [Q] dx\, dy [T_b] \tag{30}$$

$$[\bar{k}_{bm}] = [T_b]^T \iint [Q]^T [F]^T [C] [G] dx\, dy [T_m] \tag{31}$$

$$[\bar{k}_{mb}] = [\bar{k}_{bm}]^T \tag{32}$$

Evaluation of $[\bar{k}]$ is based on numerical integration using a four-point Gaussian integration which can exactly integrate for polynomial of cubic order. The matrices $[T_b]$, $[T_m]$, $[H]$, $[Q]$ and $[G]$ defined in equations (21), (22), (23), (25) and (26) are given in Appendix B.

The corresponding equations and matrices for the beam element are given in Appendix A. Element linear bending stiffness matrix $[k_b]$, membrane stiffness matrix $[k_m]$, consistent bending mass matrix $[m_b]$ and membrane mass matrix $[m_m]$ for the beam can be found in reference 55.

Element Harmonic Force Matrix

In classic continuum approach, the dynamic von Karman plate equations of motion are (refs. 2 and 3)

$$\nabla^4 \psi = E\,(w,^2_{xy} - w,_{xx}\, w,_{yy}) \tag{33}$$

$$\bar{L}(w,\psi) = \rho h w_{,tt} + D\nabla^4 w - h\,(\psi_{,yy}\, w_{,xx}$$

$$+ \psi_{,xx}\, w_{,yy} - 2\psi_{,xy}\, w_{,xy}) - F(t) = 0 \qquad (34)$$

The equation of motion for a beam with ends restrained from longitudinal movement is (ref.4)

$$\bar{L}(w) = \rho S\, w_{,tt} + EI\, w_{,xxxx} - N w_{,xx} - F(t) = 0 \qquad (35)$$

with

$$N = \frac{ES}{2L} \int w_{,x}^2\, dx \qquad (36)$$

For single mode approximate solutions, the deflection function is assumed in the form

$$w = \begin{cases} hq(t)\,\phi(x,y) & \text{, for plate} \quad (37a) \\ Rq(t)\phi(x) & \text{, for beam} \quad (37b) \end{cases}$$

where R is the radius of gyration of beam cross-section, and mode shape ϕ satisfies the related boundary conditions. Substitution of equation (37a) into equation (33), the stress function $\psi(x,y)$ is then solved from the compatibility equation (33). Application of the Galerkin procedure $\int\int \bar{L}(w,\psi)\phi(x,y)dxdy = 0$ (or $\int \bar{L}(w)\phi(x)dx = 0$ for beam) yields a modal equation in the Duffing form (refs. 4, 5 and 15 to 17)

$$mq_{,tt} + kq + \bar{k}\, q^3 = F(t) \qquad (38)$$

or in nondimensional time τ (ref. 53)

$$q_{,\tau\tau} + q + \beta q^3 = F(\tau) \tag{39}$$

When the forcing function $F(\tau)$ is simple harmonic $P_o \cos \omega\tau$, an approximate solution of equation (39) using the perturbation method is the well-known result (refs. 4, 15, 53).

$$\left(\frac{\omega}{\omega_L}\right)^2 = 1 + \frac{3}{4}\beta A^2 - \frac{P_o}{A} \tag{40}$$

With a simple elliptic forcing function $F(\tau) = BAcn(\lambda\tau, n) = Bq$ as the external excitation to the Duffing system, an elliptic response (refs. 4, 5, 15 to 17, and 53)

$$q = A\, cn(\lambda\tau, n) \tag{41}$$

is obtained as an exact solution of equation (39), where B is the non-dimensional forcing amplitude factor, λ and n are the circular frequency and the modulus of the Jacobian elliptic function, and $A = w_{max}/h$ (w_{max}/R for beam) is the amplitude. By expanding the elliptic forcing function into the Fourier series and comparing the orders of magnitude of the various harmonic components, Hsu (ref. 53) showed that the single harmonic forcing function $P_o \cos \omega\tau$ is the first order approximation of the elliptic forcing function $BAcn(\lambda\tau, n)$. Also the first order approximation of the elliptic response of equation (39) yields the same frequency-amplitude relations of equation (40) as the perturbation solution. In obtaining the exact elliptic response of equation (39), the excitation force $F(\tau) = Bq$ is treated as a linear spring in the Duffing equation

$$q_{,\tau\tau} + (1-B)q + \beta q^3 = 0 \tag{42}$$

This linear spring force Bq posses a potential energy of $V = Bq^2/2$. The potential energy of an element subjected to a uniform harmonic forcing function can thus be approximated by

$$V = \begin{cases} \frac{B}{2} \iint w^2 \, dxdy & \text{, for plate} \quad (43a) \\ \frac{B}{2} \int w^2 \, dx & \text{, for beam} \quad (43b) \end{cases}$$

An examination of equations (11) and (43) indicates that the harmonic force matrix for the plate or beam element under uniform loading $F_o \cos\omega t$ is

$$[p] = \begin{cases} \frac{cF_o}{A\rho h^2} [m_b] & \text{, for plate} \quad (44a) \\ \frac{cF_o}{AR\rho S} [m_b] & \text{, for beam} \quad (44b) \end{cases}$$

The actual applied distributed force intensity F_o (N/m^2 or psi for plate, N/m or lb/in. for beam) is related to the dimensionless forcing parameter P_o and the dimensionless forcing amplitude factor B by

$$B = \frac{P_o}{A} = \begin{cases} \frac{cF_o}{A\rho h^2 \omega_L^2} & \text{, for plate} \quad (45a) \\ \frac{cF_o}{AR\rho S\omega_L^2} & \text{, for beam} \quad (45b) \end{cases}$$

where

$$c = \frac{\iint_{(\text{Loaded elements})} \phi dxdy}{\iint_{(\text{Total plate area})} \phi^2 dxdy} \tag{46}$$

For plates under uniformly distributed force over entire plate

$$c = \frac{\iint_{(\text{Total plate})} \phi dxdy}{\iint_{(\text{Total plate area})} \phi^2 dxdy} \tag{47}$$

which is simply the ratio of volumes (area) under plate (beam) mode shape and square of mode shape. The harmonic force matrix of equation (44) depends on the plate amplitude $A = w_{max}/h$ (w_{max}/R for beam) and P_o (or F_o).

Equation of Motion and Solution Procedures

The application of the Lagrange's equation leads to the equation of motion for the present rectangular plate and beam elements under the influences of inertia, elastic, large deflection and uniform harmonic excitation force as

$$\begin{bmatrix} [m_b] & 0 \\ 0 & [m_m] \end{bmatrix} \{\ddot{\delta}\} + \left(\begin{bmatrix} [k_b] & 0 \\ 0 & [k_m] \end{bmatrix} + \begin{bmatrix} [\bar{k}_b] & [\bar{k}_{bm}] \\ [\bar{k}_{mb}] & 0 \end{bmatrix} - \begin{bmatrix} [p] & 0 \\ 0 & 0 \end{bmatrix} \right) \{\delta\} = 0 \tag{48}$$

The coupling between bending and membrane stretching is evident by the presence of $[\bar{k}_{bm}]$ and $[\bar{k}_{mb}]$ matrices in equation (48). Nonlinear free vibration is a special case of the general nonlinear forced vibration problem with P_o or $[p] = 0$ in equation (48).

By assembling the finite elements and applying the kinematic boundary conditions, the equations of motion for the linear free vibration of a given plate or beam may be written as

$$\omega_L^2 [M] \{\phi\}_o = [K] \{\phi\}_o \tag{49}$$

where $[M]$ and $[K]$ denote the system mass and linear stiffness matrices, respectively, ω_L is the fundamental linear frequency, and $\{\phi\}_o$ denotes the corresponding linear mode shape normalized to unit value of the largest component. The deflection $w_{max}\{\phi\}_o$ is then used to obtain the element nonlinear stiffness matrix $[\bar{k}]$ through equations (25 and 30 to 32). The element harmonic force matrix is obtained through equation (44) for given P_o and A. The nonlinear forced vibration response is approximated by a linearized eigenvalue equation of the form

$$\omega^2 [M] \{\phi\}_1 = ([K] + [\bar{K}] - [P]) \{\phi\}_1 \tag{50}$$

where ω is the fundamental nonlinear frequency associated with dimensionless amplitude A and force parameter P_o, and $\{\phi\}_1$ is the corresponding normalized mode shape of the first iteration. The iterative process can now be repeated with $w_{max}\{\phi\}_1$ until a convergence criterion is satisfied.

Convergence and Strains

The three displacement convergence criteria proposed by Bergan and Clough (ref. 56) for nonlinear static and post-buckling analyses are employed in the nonlinear free and forced vibrational problems. The three displacement norms are the modified absolute norm, modified Euclidean norm and the maximum norm. They are defined as

$$||\xi||_{abs} = \frac{1}{n} \sum_{i=1}^{n} \left| \frac{\Delta\phi_i}{\phi_{i,ref}} \right| \tag{51}$$

$$||\xi||_{Euc} = \left[\frac{1}{n} \sum_{i=1}^{n} \left| \frac{\Delta\phi_i}{\phi_{i,ref}} \right|^2 \right]^{1/2} \tag{52}$$

and

$$||\xi||_{max} = \max_i \left| \frac{\Delta\phi_i}{\phi_{i,ref}} \right| \tag{53}$$

where n is the total degrees-of-freedom of the beam or plate structure, $\Delta\phi_i$ is the change in displacement component i during interation cycle. The reference displacement $\phi_{i,ref}$ is the largest displacement component of the corresponding type (ref. 56). In addition a frequency norm is also introduced in the present study and it is defined as

$$||\xi||_{freq} = \left| \frac{\Delta\omega}{\omega} \right| \tag{54}$$

where $\Delta\omega$ is the change in nonlinear frequency during the iteration cycle. A typical plot of the four norms versus number of iterations for a simply supported beam of slenderness ratio $L/R = 100$ with immovable end supports subjected to a uniform harmonic force of $P_o = 2.0$ at $A = w_{max}/R = 4.0$ is shown in figure 2. Figure 3 shows the convergence characteristics of a simply supported square plate of length-to-thickness ratio $a/h = 240$ with immovable inplane edges ($u = 0$ at $x = 0$ and a, $v = 0$ at $y = 0$ and a) subjected to a uniform harmonic force of forcing parameter $P_o = 0.2$ at $A = w_{max}/h = 1.0$. All four norms exhibit the important behavior of straightness and parallelism as described in reference 56. Therefore, there is no great significance as to what specific norm is being used since they are parallel, and also an upper bound or maximum error on displacement and frequency convergences can be estimated since they are straight. The results presented in this report, convergence is considered achieved whenever anyone of the norms reaches a value of 10^{-5}.

Once the convergence is satisfied, the membrane and bending strain components at the four nodes of the plate element can be obtained from the plate deflection and equations (2), (3), (21) to (23) and (25). They are

$$\begin{Bmatrix} \varepsilon_x \\ \varepsilon_y \\ \gamma_{xy} \end{Bmatrix}_m = \left[[F][Q] \,\middle|\, [G] \right] \begin{bmatrix} T_b & 0 \\ 0 & T_m \end{bmatrix} \begin{Bmatrix} \delta_b \\ \delta_m \end{Bmatrix} \tag{55}$$

$$\begin{Bmatrix} \varepsilon_x \\ \varepsilon_y \\ \gamma_{xy} \end{Bmatrix}_b = z\,[H][T_b]\,\{\delta_b\} \tag{56}$$

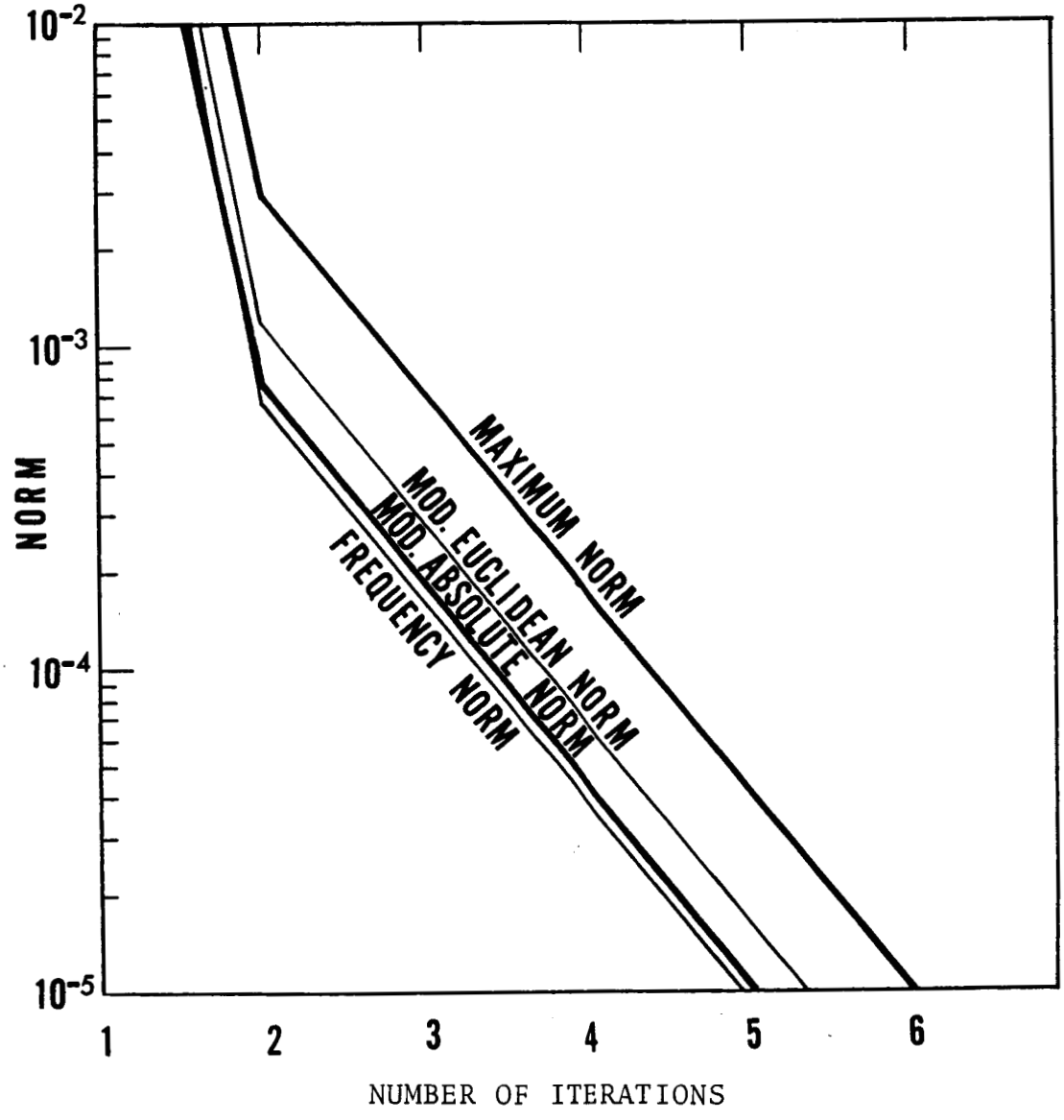

Figure 2. Typical convergence characteristics of beams.

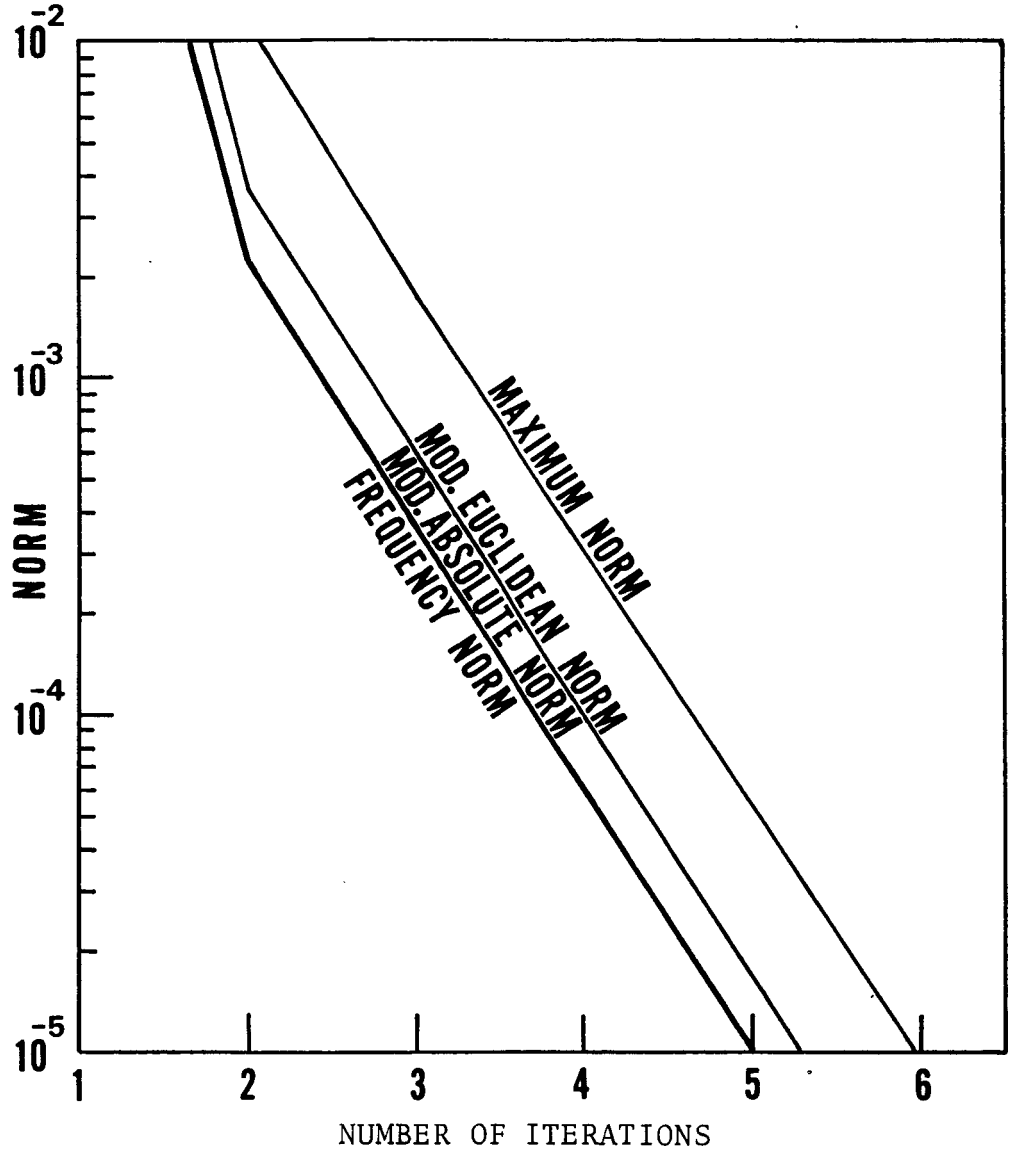

Figure 3. Typical convergence characteristics of plates.

Maximum normal strain is evaluated with z at the top or bottom surfaces ($z = \pm h/2$). The corresponding strain expressions for the beam element are given in Appendix A.

RESULTS AND DISCUSSION

Beams

Improved Nonlinear Free Vibration

The fundamental frequency ratios ω/ω_L of free vibration at various amplitude $A = w_{max}/R$ for a simply supported beam ($L/R = 100$) with both ends immovable ($u = 0$ at $x=0$ and L) are shown in table I. Due to symmetry, only one-half of the beam which is divided equally into six elements is used. Finite element results with and without considering longitudinal deformation and inertia (LDI) in the analyses are both given. It shows that the effects of improved finite element results by including LDI in the formulation are to reduce the nonlinearity. The elliptic function solution (refs. 1, 4 and 53) is also given to demonstrate the closeness of the earlier finite element results without LDI. Raju et al. (ref. 57) used the Rayleigh-Ritz method in investigation of the effects of inplane deformation and inertia on large amplitude flexual vibration of slender beams. Appropriate frequency-amplitude relationship using Rayleigh-Ritz method is also given in table I. In Rayleigh-Ritz method, accuracy of the frequency depends heavily on the assumed beam deflection functions (usually linear mode shapes). The present finite element approach, the beam deflection approachs the "true" nonlinear beam deflection through an iterative process. The final beam deflection, therefore, would be more accurate, and also the frequency ratios obtained.

TABLE I. FREE VIBRATION FREQUENCY RATIOS ω/ω_L FOR A SIMPLY SUPPORTED BEAM WITH IMMOVABLE AXIAL ENDS.

$A = \frac{w_{max}}{R}$	Without LDI[a]			With LDI (L/R = 100)		
	Elliptic Function Solution (ref. 1)	Earlier Finite Element		Rayleigh Ritz Solution (ref. 57)	Present Finite Element	
		First Iteration	Final Result		First Iteration	Final Result
1.0	1.0892	1.0895	1.0888	1.0607	1.0613	1.0613(3)[b]
2.0	1.3178	1.3203	1.3119	1.2246	1.2270	1.2269(4)
3.0	1.6257	1.6295	1.6022	1.4573	1.4620	1.4617(4)
4.0	1.9760	1.9761	1.9216	1.7309	1.7383	1.7375(6)
5.0	2.3501	2.3396	2.2544	2.0289	2.0393	2.0378(7)

a. Longitudinal deformation and inertia.
b. Number inside parenthesis denotes the number of iterations to get a converged solution.

Nonlinear Forced Response of Beams with Immovable Ends

Table II shows the frequency ratios of the same simply supported beam (L/R = 100) subjected to a uniform harmonic force of $P_o = 2.0$. It demonstrates the closeness between the earlier finite element results without LDI, the simple elliptic response (refs. 4 and 53) and the perturbation solution of equation (40). The present improved finite element results indicate clearly that the effects of LDI are to reduce the nonlinearity as in the free vibration case. Similar results of a clamped beam (L/R = 100) with immovable axial end supports subjected to a uniform harmonic force of $P_o = 1.0$ are also given in table II. The present finite element results of a slender beam (L/R = 100) to uniform harmonic excitation of $P_o = 0$, 1.0 and 2.0 are given in figures 4 and 5 for simply supported and clamped boundary conditions, respectively.

Table III shows the maximum strain-amplitude relation for the simply support and clamped beams (L/R = 100) with immovable axial end supports. These results are also shown in figure 6 for absolute value. The service life can thus be estimated from the maximum strain and frequency in conjunction with the corresponding material strain-cycle fatigue data (S-N curve). This is not possible if small deflection free vibration analysis is employed.

Nonlinear Forced Response of Beams with Movable End-Support

Figures 7(a) and (b) show the nondimensional amplitude A versus ω/ω_L for a simply supported beam of slenderness ratio L/R = 100 and 20, respectively. One of the end supports (x = L) is assumed to be free to move in the axial direction. For a highly slender beam (L/R > 100), tne hard spring type nonlinearity due to large deflection is so small as shown in figure 7(a), therefore, it can be practically neglected. Longitudinal deformation

Table II. FORCED VIBRATION FREQUENCY RATIOS ω/ω_1 FOR A SIMPLY SUPPORTED AND A CLAMPED BEAM WITH IMMOVABLE AXIAL ENDS.

$A = \frac{w_{max}}{R}$	Without LDI[a]				With LDI
	Simple Elliptic Response (refs. 4 and 53)	Perturbation Solution	Earlier Finite Element		Present Finite Element Final Result
			First Iteration	Final Result	
Simply Supported Beam Subjected to $P_0 = 2.0$ ($F_0 = 2.31506 \times 10^5$ N/m)					
- 1.0	1.7852	1.7854	1.7852	1.7856	1.7682(3)[b]
± 2.0	0.8472 1.6557	0.8660 1.6583	0.8621 1.6563	0.8460 1.6512	0.7108(4) 1.5829(4)
± 3.0	1.4003 1.8217	1.4216 1.8314	1.4102 1.8226	1.3760 1.8002	1.2123(4) 1.6743(4)
± 4.0	1.8413 2.1013	1.8708 2.1213	1.8453 2.0988	1.7846 2.0495	1.5871(6) 1.8759(6)
± 5.0	2.2606 2.4361	2.2995 2.4673	2.2525 2.4236	2.1619 2.3432	1.9371(7) 2.1337(7)
Clamped Beam Subjected to $P_0 = 1.0$ ($F_0 = 5.73862 \times 10^5$ N/m)					
± 1.0	0.2118 1.4307	0.2165 1.4307	0.2096 1.4297	0.2091 1.4297	0.1772(3) 1.4251(3)
± 2.0	0.8279 1.2987	0.8292 1.2990	0.8215 1.2942	0.8203 1.2936	0.7905(4) 1.2743(4)
± 3.0	1.0401 1.3232	1.0433 1.3248	1.0279 1.3127	1.0239 1.3099	0.9726(5) 1.2694(5)
± 4.0	1.2183 1.4101	1.2247 1.4142	1.1979 1.3910	1.1888 1.3836	1.1151(6) 1.3197(6)
± 5.0	1.3938 1.5322	1.4042 1.5401	1.3619 1.5016	1.3457 1.4874	1.2513(8) 1.4014(8)

a. Longitudinal deformation and inertia.
b. Number inside parenthesis denotes the number of iterations to get a converged solution.

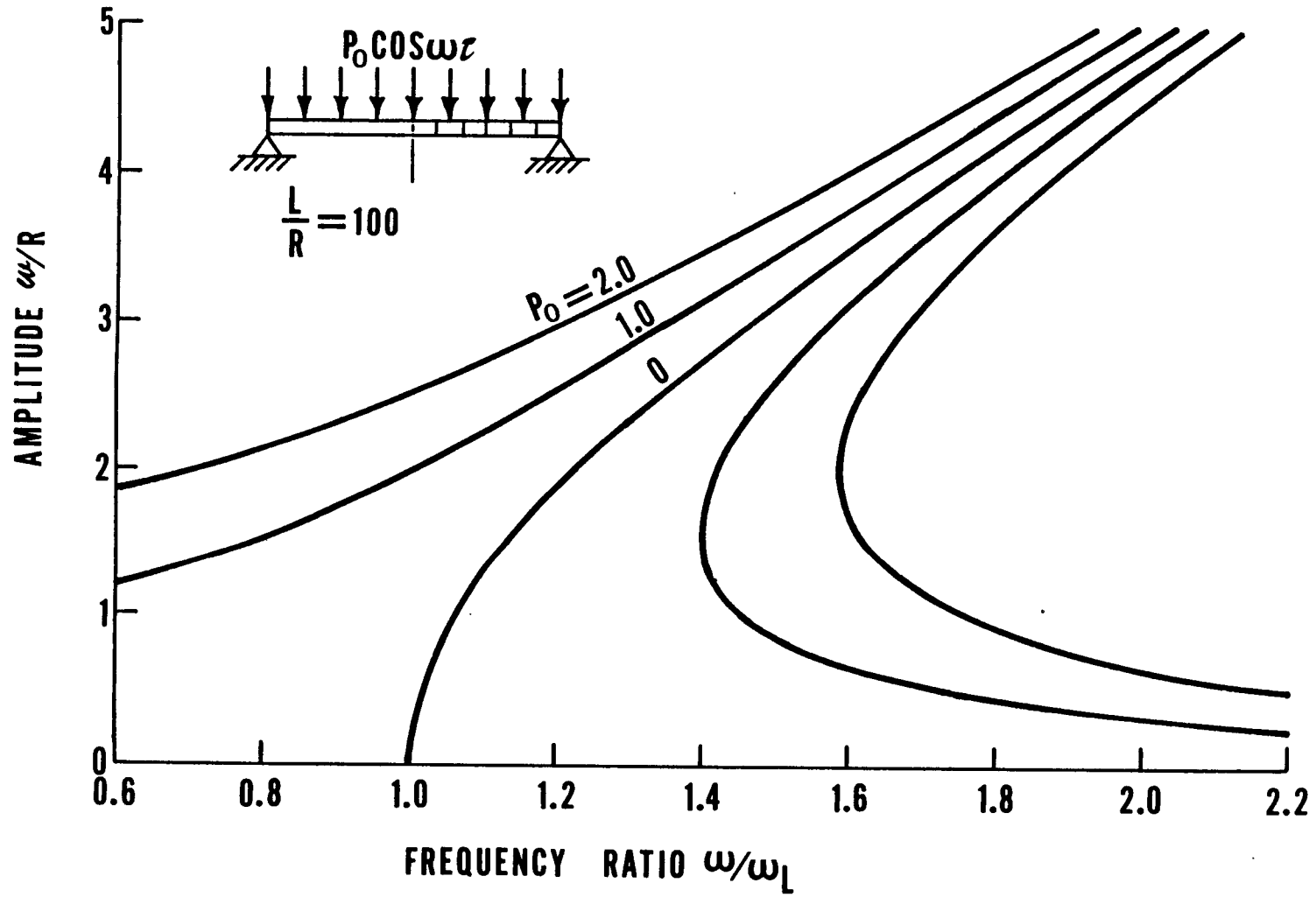

Figure 4. Amplitude versus frequency for a simply supported beam with immovable axial end supports at uniform P_o = 0, 1.0 and 2.0.

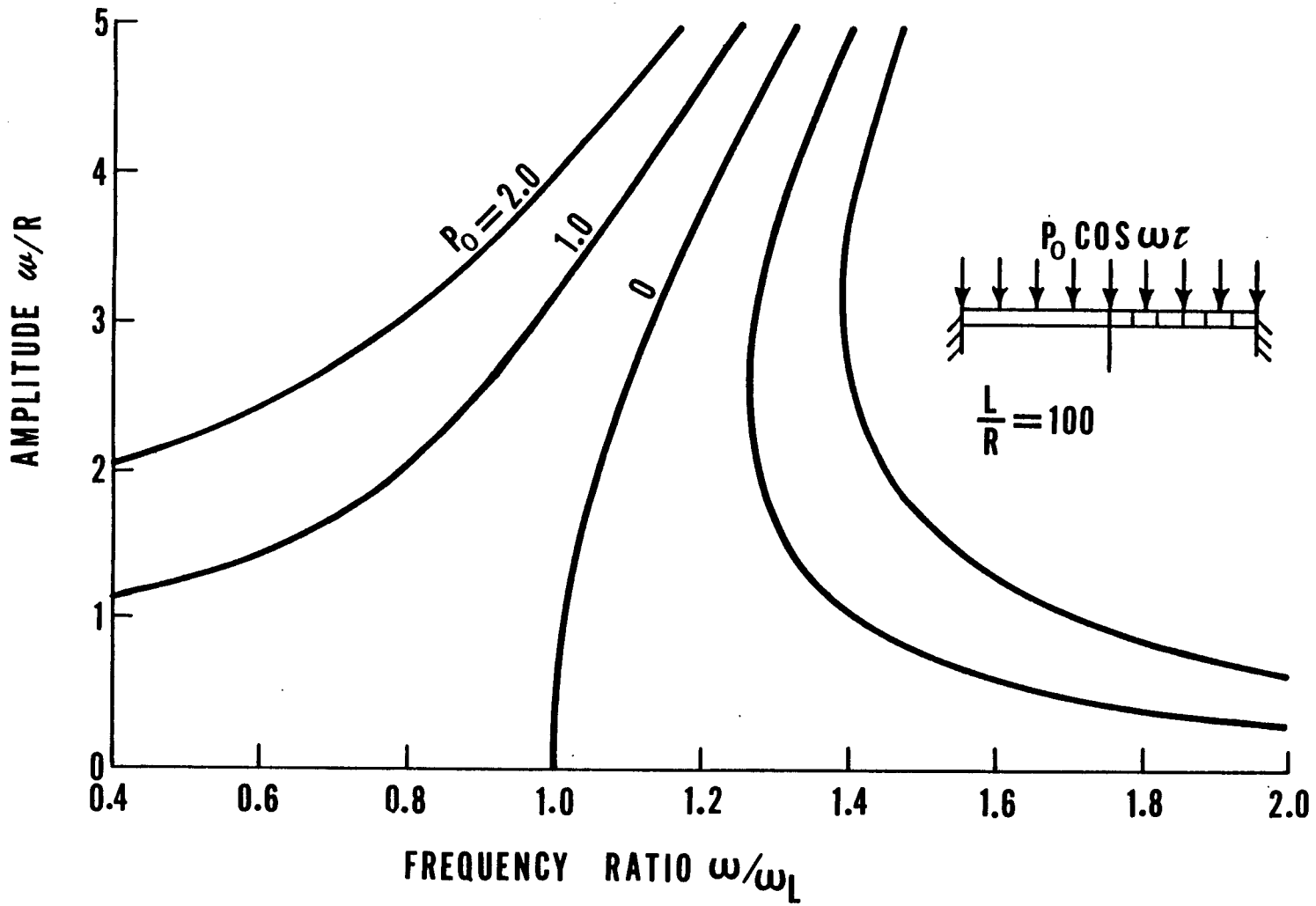

Figure 5. Amplitude versus frequency for a clamped beam with immovable axial end supports at uniform P_o = 0, 1.0 and 2.0.

Table III. MAXIMUM STRAIN FOR BEAMS WITH IMMOVABLE AXIAL ENDS (L/R = 100) INCLUDING INPLANE DEFORMATION AND INERTIA.

$A = \frac{w_{max}}{R}$	Simply-Support	Clamped
1.0	1.955×10^{-3}	-4.741×10^{-3}
2.0	4.386×10^{-3}	-9.367×10^{-3}
3.0	7.292×10^{-3}	-14.107×10^{-3}
4.0	10.676×10^{-3}	-19.169×10^{-3}
5.0	14.535×10^{-3}	-24.726×10^{-3}

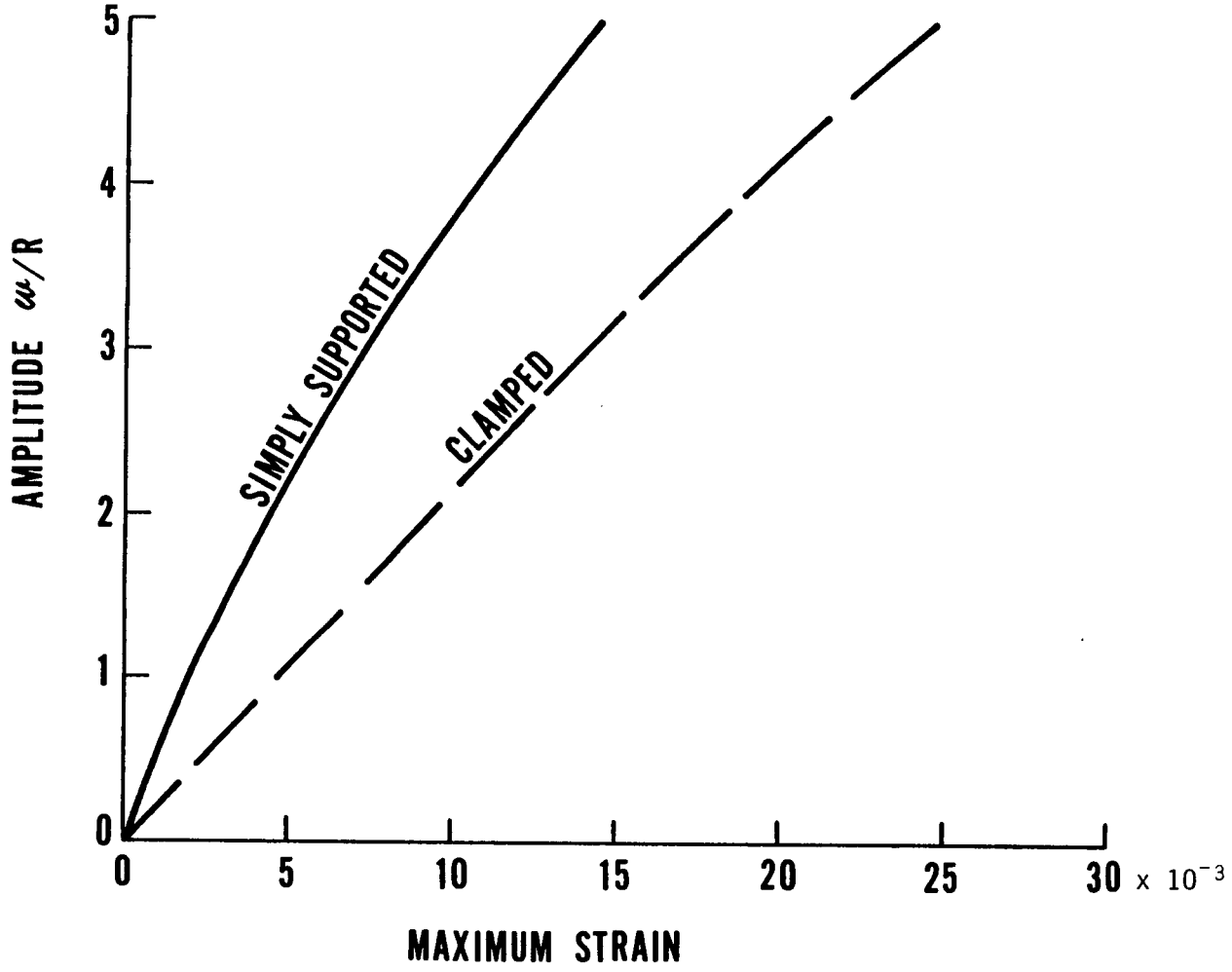

Figure 6. Amplitude versus maximum strain for simply supported and clamped beams with immovable axial end supports.

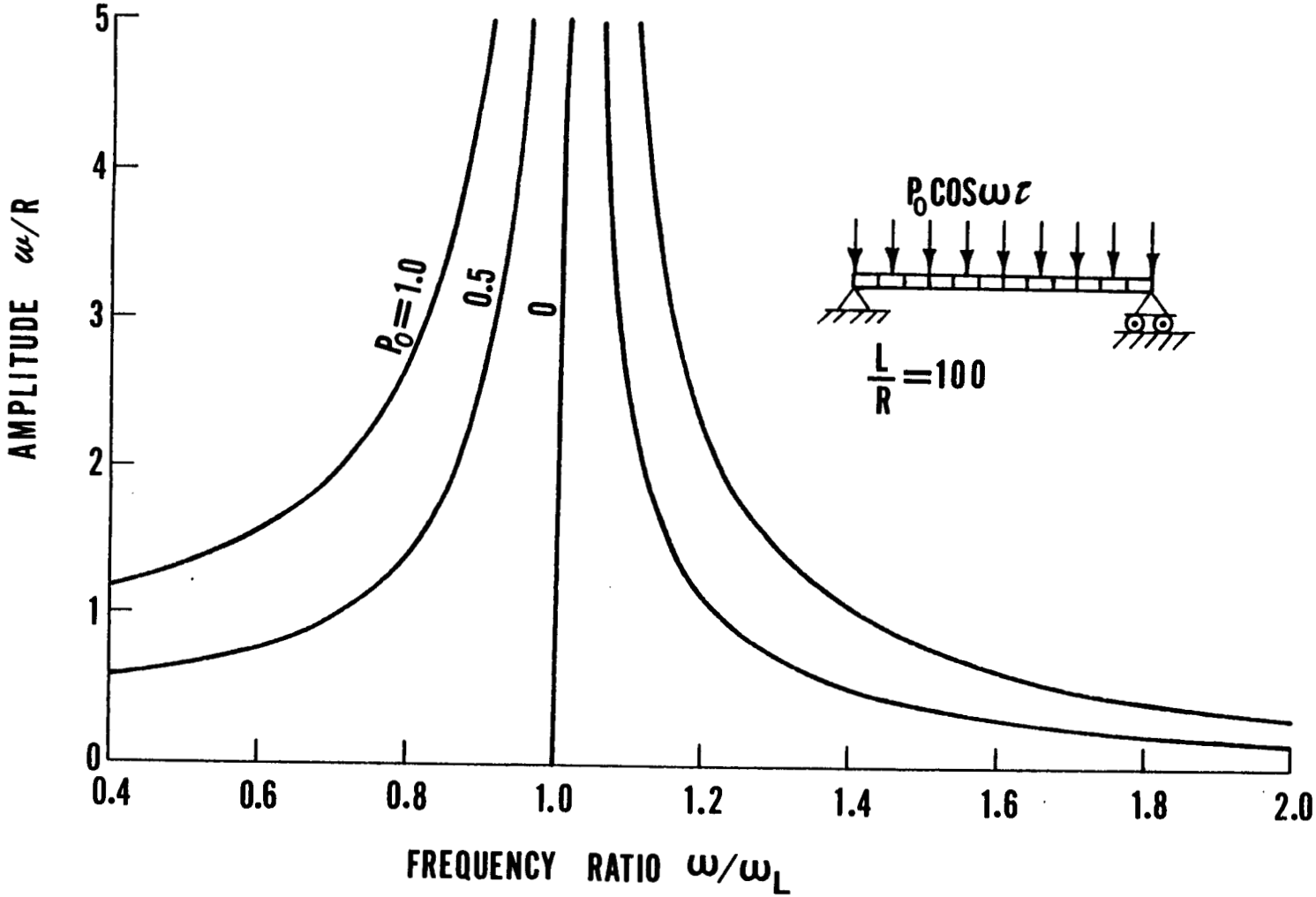

(a) Slenderness ratio L/R = 100

Figure 7. Amplitude versus frequency for a simply supported beam with a movable axial end support at uniform P_o = 0, 0.5 and 1.0.

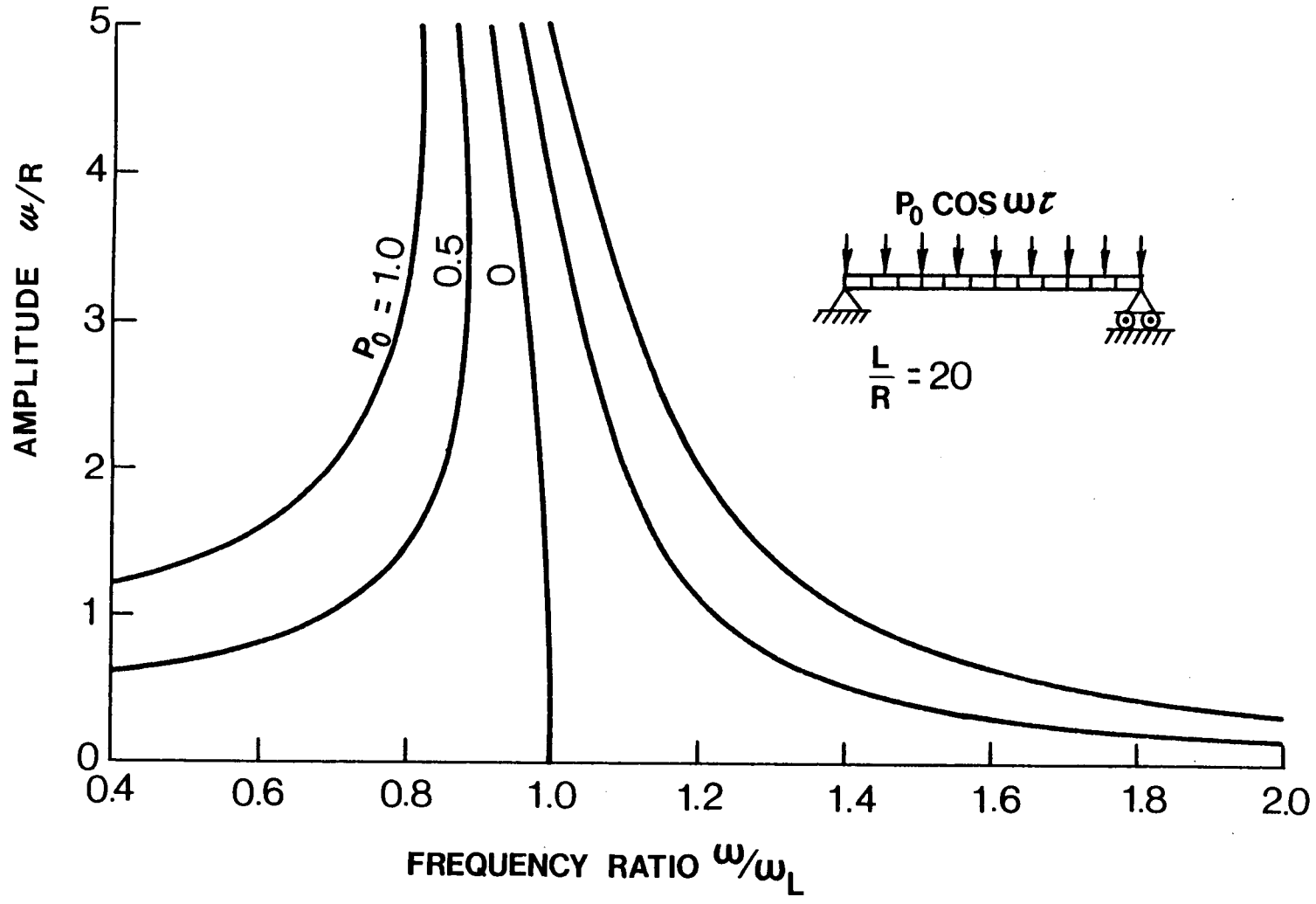

(b) Slenderness ratio L/R = 20.

Figure 7. Concluded.

and inertia effects are more pronounced in a short beam than a long one. As a consequence, the reduction of nonlinearity due to longitudinal deformation and inertia, from the nearly small deflection linear case in figure 7(a), leads to a situation that the beam eventually exhibits slightly soft spring type nonlinearity as shown in figure 7(b). Atluri (ref. 58) also obtained similar nonlinearity of softening type in his investigation.

Concentrated Harmonic Force

The element harmonic force matrix [p] derived in equation (44) is for uniformly distributed load over the element. The method used here to simulate a concentrated force is to let the length of the loaded beam element become smaller and smaller. This is demonstrated by a concentrated force applied at the center of a simply supported beam (L/R = 100) with immovable inplane edges. The magnitude of the concentrated force is equal to the same beam under a uniform distributed load of $P_o = 1.0$ ($F_o = 1.158 \times 10^5$ N/m or 661 lb/in.) over the entire beam. Therefore, the uniform loading of the loaded element for the concentrated case is $F_o = 115.8 \times L/d$ kN/m where d is the length of the loaded beam element. The constant c is given in equation (46). The results are given in table IV at various d/L ratios and in figure 8 for d/L = 5%. The elliptic function and perturbation solutions (without inplane deformation and inertia) are also given in table IV. It is shown that the concentrated force case is approximately 1.6 times as much severe as the uniform distributed force for the case studied.

Table IV. CONVERGENCE OF FREQUENCY RATIOS ω/ω_l WITH LOADED LENGTH d FOR A SIMPLY SUPPORTED BEAM (L/R = 100) WITH IMMOVABLE INPLANE EDGES SUBJECTED TO A CONCENTRATED FORCE F_0 = 115.8 x L/d kN/m AT THE CENTER.

$A = \frac{w_{max}}{R}$	Without LDI*		Finite Element with LDI at (d/L)%			
	Elliptic Solution	Perturbation Solution	20	5	1	0.5
- 1.0	1.6607	1.6608	1.6316	1.6411	1.6423	1.6425
- 2.0	.9695	.9821	.8585	.8506	.8497	.8497
	1.5894	1.5923	1.5077	1.5134	1.5143	1.5143
- 3.0	1.4519	1.4710	1.2742	1.2718	1.2717	1.2717
	1.7815	1.7920	1.6273	1.6317	1.6325	1.6326
- 4.0	1.8711	1.8993	1.6229	1.6226	1.6229	1.6229
	2.0751	2.0959	1.8446	1.8485	1.8494	1.8495
5.0	2.2801	2.3181	1.9606	1.9615	1.9620	1.9621
	2.4179	2.4498	2.1116	2.1154	2.1164	2.1165

*Longitudinal deformation and inertia.

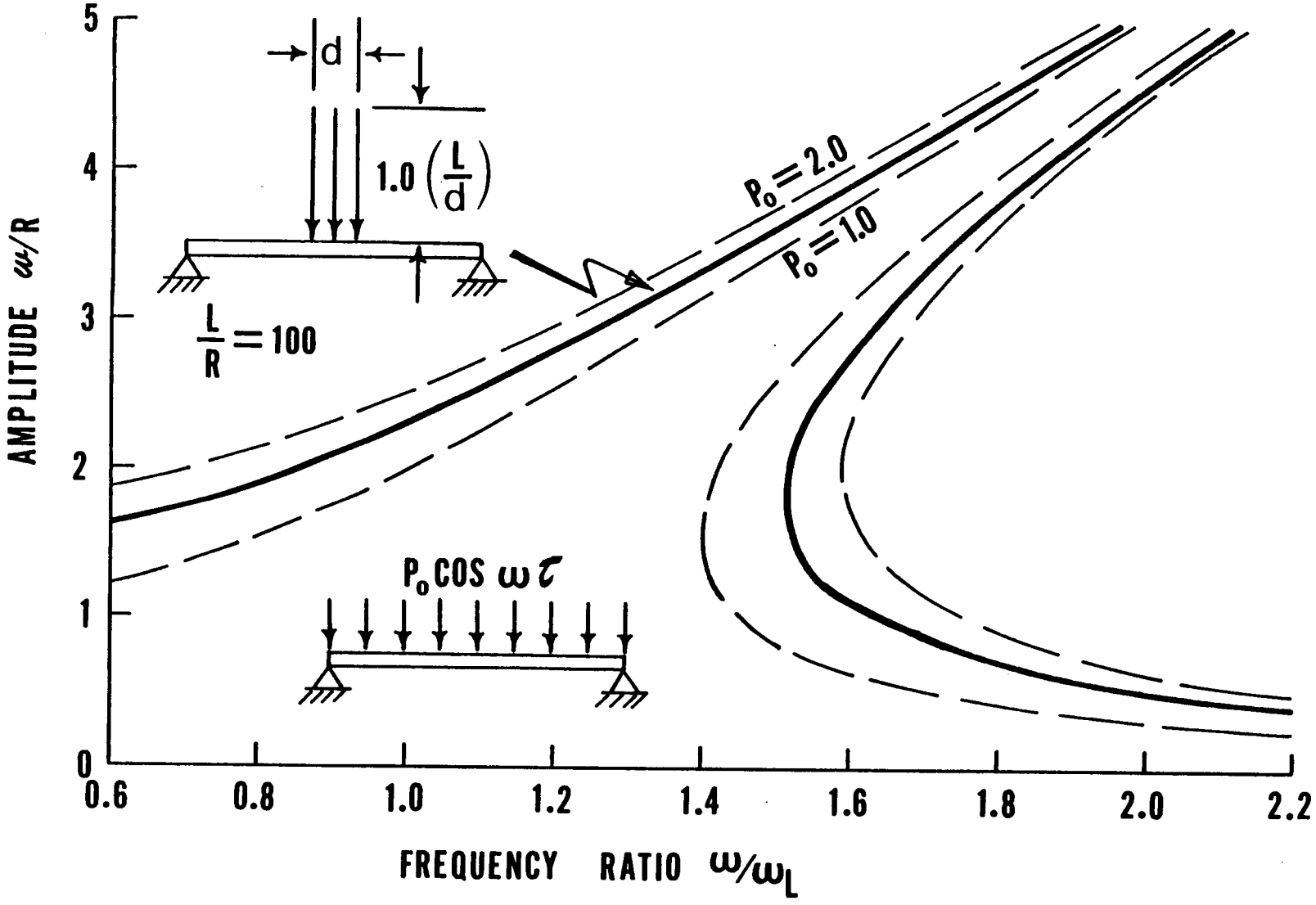

Figure 8. Amplitude versus frequency for a simply supported beam with immovable axial end supports under concentrated loading.

Table VI. CONVERGENCE OF FREQUENCY RATIOS ω/ω_1 WITH GRIDWORK REFINEMENT FOR A SIMPLY SUPPORT SQUARE PLATE ($a/h = 240$) WITH IMMOVABLE INPLANE Edge Subjected to $P_0 = 0.2$.

$A = \frac{w_{max}}{h}$	Gridwork		
	2 x 2 (4 Elements)	3 x 3 (9 Elements)	4 x 4 (16 Elements)
± 0.2	0.1645(3)* 1.4248(3)	0.1643(3) 1.4238(3)	0.1636(3) 1.4237(3)
± 0.4	0.7815(3) 1.2697(3)	0.7800(3) 1.2682(3)	0.7792(3) 1.2677(3)
± 0.6	0.9576(4) 1.2588(4)	0.9544(4) 1.2560(4)	0.9530(4) 1.2550(4)
± 0.8	1.0937(5) 1.3026(5)	1.0886(5) 1.2981(5)	1.0865(5) 1.2963(5)
± 1.0	1.2242(5) 1.3781(5)	1.2171(6) 1.3717(6)	1.2143(5) 1.3691(5)

*Number in parenthesis denotes the number of iterations to get a congerged solution.

Plates

Improved Nonlinear Free Vibration

The fundamental frequency ratios ω/ω_L of free vibration at various amplitude $A = w_{max}/h$ for simply supported square (a/h = 240) and rectangular (a/b = 2 and a/h = 480) plates with immovable inplane edges (u=0 at x = 0 and a, v=0 at y=0 and b) are shown in table V. Due to symmetry, only one quarter of the plate modelled with 9 (or 3 x 3 gridwork) elements of equal sizes is used. Both finite element results with and without inplane deformation and inertia (IDI) are given. It shows that the improved finite element results by including IDI in the formulation are to reduce the nonlinearity. The elliptic function solution and perturbation solution (with inplane deformation only, refs. 4 and 53) are also given to demonstrate the closeness of the earlier finite element results without IDI. Raju et al. (ref. 57) used the Rayleigh-Ritz method in investigation of the effects of IDI on large amplitude free flexural vibration of thin plates. The linear mode shape is very close to the nonlinear mode shape for the simply supported case. Therefore, the Rayleigh-Ritz solution demonstrates a good result compared to the present improved finite element solution.

Convergence with Gridwork Refinement

Table VI shows the frequency ratios for a simply supported square plate (a/h = 240) with immovable inplane edges subjected to a uniform harmonic force of $P_o = 0.2$ with three finite element gridwork refinements. Only one quarter of the plate was used in the analysis due to symmetry. Examination of the results shows that the present finite element formulation exhibits excellent convergence characteristics. Therefore, a 3 x 3 (or 9 elements) in a quarter of plate was used in modeling the plates in the

Table V. FREE VIBRATION FREQUENCY RATIOS ω/ω_L FOR A SIMPLY SUPPORTED PLATE WITH IMMOVABLE INPLANE EDGES.

$A = \frac{w_{max}}{h}$	Without IDI[a]	With Inplane Deformation (No Inertia)		With IDI	
	Finite Element Result	Elliptic Function Result (refs. 4 and 53)	Perturbation Solution	Rayleigh Ritz Result (ref. 57)	Present Finite Element Result
Square Plate (a/h = 240)					
0.2	1.0185(3)[b]	1.0195	1.0196	1.0149	1.0134(3)
0.4	1.0716(3)	1.0757	1.0761	1.0583	1.0528(3)
0.6	1.1533(4)	1.1625	1.1642	1.1270	1.1154(4)
0.8	1.2565(6)	1.2734	1.2774	1.2166	1.1979(5)
1.0	1.3752(7)	1.4024	1.4097	1.3230	1.2967(6)
Rectangular Plate (a/b = 2, a/h = 480)					
0.2	1.0238(3)	1.0241	1.0241	1.0177	1.0168(3)
0.4	1.0918(4)	1.0927	1.0933	1.0690	1.0658(4)
0.6	1.1957(6)	1.1975	1.1998	1.1493	1.1439(5)
0.8	1.3264(8)	1.3293	1.3347	1.2533	1.2467(6)
1.0	1.4762(11)	1.4808	1.4903	1.3753	1.3701(8)

a. Inplane deformation and inertia.
b. Number inside parenthesis denotes the number of iterations to get a converged solution.

remainder of the nonlinear forced responses presented unless otherwise specified.

Nonlinear Forced Response of Plates with Immovable Inplane Edges

Table VII shows the frequency ratios ω/ω_L for simply supported and clamped square plates (a/h = 240) subjected to a uniform harmonic force of $P_o = 0.2$. It demonstrates the closeness between the earlier finite element formulation without IDI, the simple elliptic response (refs. 4 and 53) and the perturbation solution (with inplane deformation only). The present improved finite element results indicate clearly that the effects of IDI are to reduce the nonlinearity. The present finite element results of a square plate (a/h = 240) to uniform harmonic excitation of $P_o = 0$, 0.1 and 0.2 are given in figures 9 and 10 for simply supported and clamped boundary conditions, respectively.

Nonlinear Forced Response of Plates with Movable Inplane Edges

The dimensionless amplitude A versus the fundamental frequency ratio ω/ω_L for a simply supported square plate (a/h = 240) with movable inplane edges subjected to uniform harmonic load $P_o = 0$, 0.1 and 0.2 is shown in figure 11. The nonlinearity is greatly reduced with the inplane edges no longer restrained as compared to the case of immovable inplane edges in figure 9.

Concentrated Harmonic Force

Application of the present finite element to the case of a concentrated force is to let the area of the loaded element becoming smaller and smaller. It is demonstrated by a concentrated force applied at the center of a simply supported square plate (a/h = 240) with immovable inplane edges. The magni-

Table VII. FORCED VIBRATION FREQUENCY RATIOS ω/ω_1 FOR A SQUARE PLATE (a/h = 240) WITH IMMOVABLE INPLANE EDGES SUBJECTED TO P_o = 0.2.

$A = \frac{w_{max}}{h}$	Simple Elliptic Response (refs. 4 and 53)	Perturbation Solution	Finite Element	
			Without IDI[a]	With IDI
Simply Supported				
± 0.2	0.1944 1.4281	0.1987 1.4281	0.1932(3)[b] 1.4274(3)	0.1643(3) 1.4238(3)
± 0.4	0.8102 1.2874	0.8111 1.2876	0.8052(3) 1.2839(3)	0.7800(3) 1.2682(3)
± 0.6	1.0084 1.2983	1.0110 1.2995	0.9984(4) 1.2898(4)	0.9544(4) 1.2560(4)
± 0.8	1.1703 1.3686	1.1755 1.3718	1.1528(6) 1.3524(6)	1.0886(5) 1.2981(5)
± 1.0	1.3283 1.4726	1.3369 1.4789	1.3004(7) 1.4460(7)	1.2171(6) 1.3717(6)
Clamped				
± 0.2	0.1200 1.4195	0.1227 1.4195	0.1180(2) 1.4195(2)	0.1033(3) 1.4183(3)
± 0.4	0.7483 1.2490	0.7438 1.2491	0.7459(3) 1.2477(3)	0.7372(4) 1.2426(4)
± 0.6	0.8951 1.2117	0.8956 1.2119	0.8905(4) 1.2083(4)	0.8746(4) 1.1966(4)
± 0.8	0.9941 1.2203	0.9954 1.2210	0.9863(5) 1.2137(5)	0.9617(5) 1.1938(5)
± 1.0	1.0822 1.2540	1.0845 1.2555	1.0700(6) 1.2429(6)	1.0362(5) 1.2140(5)

a. Inplane deformation and inertia.
b. Number inside parenthesis denotes the number of iterations to get a converged solution.

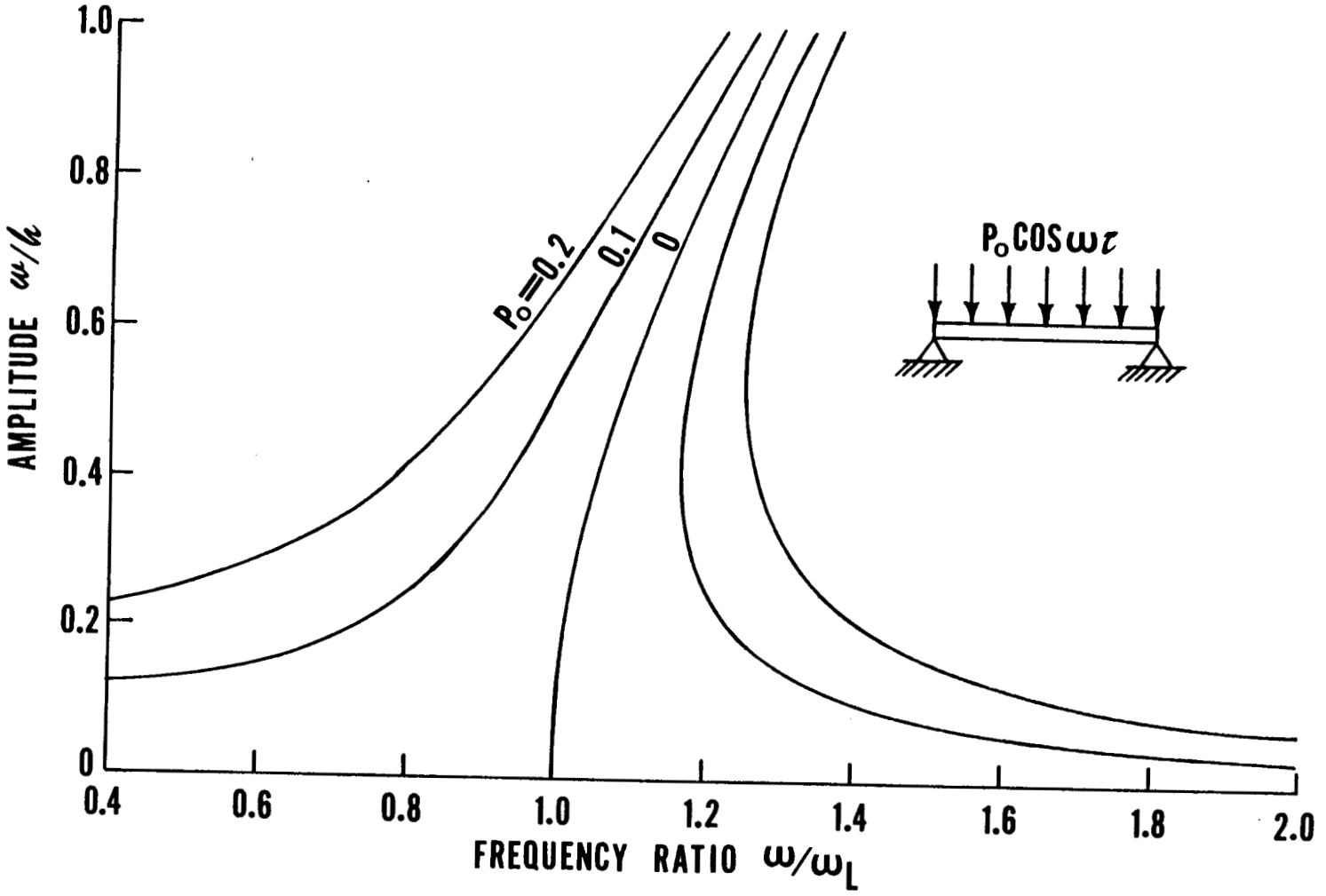

Figure 9. Amplitude versus frequency for a simply supported square plate (a/h = 240) with immovable inplane edges at P_o = 0, 0.1 and 0.2.

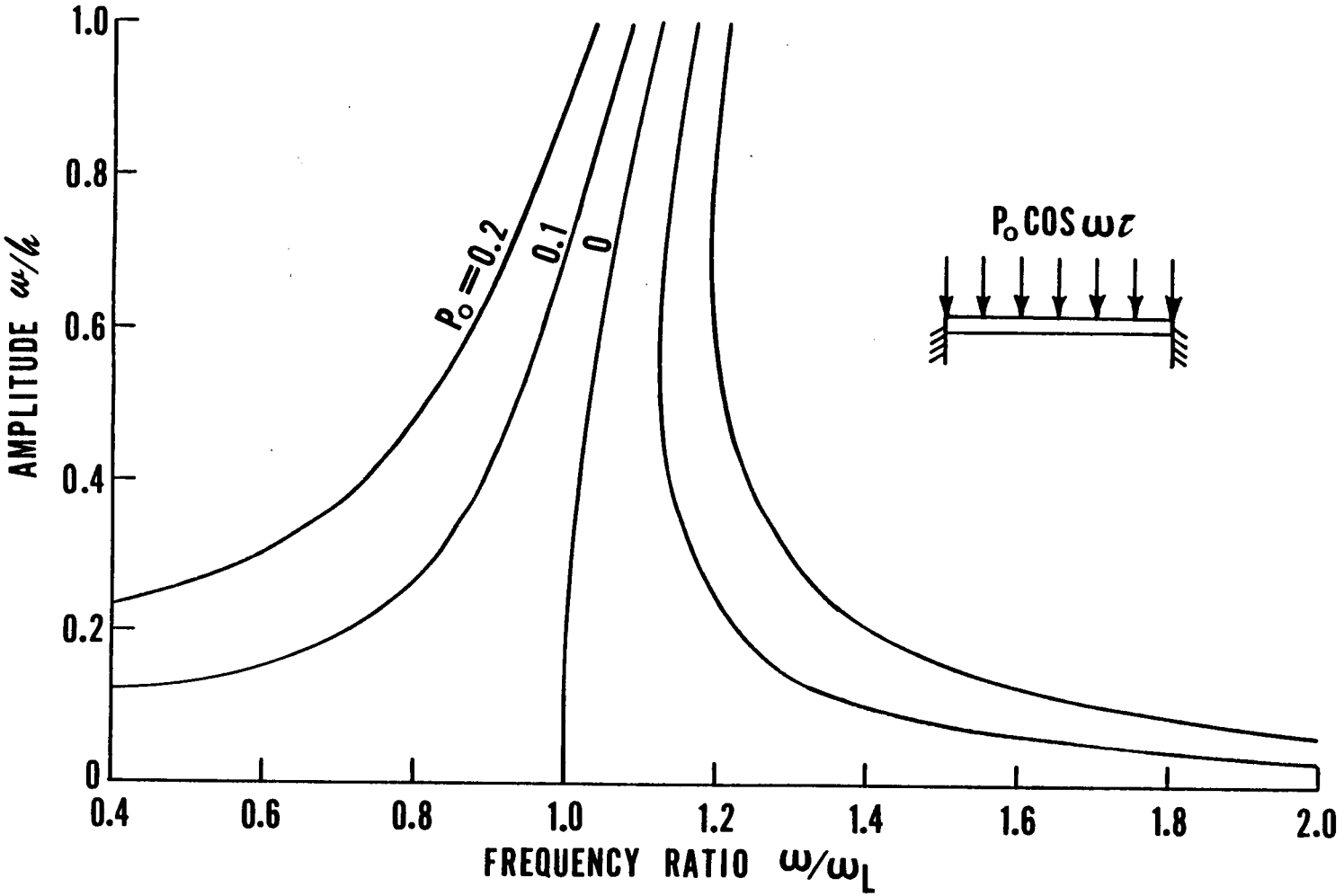

Figure 10. Amplitude versus frequency for a clamped square plate (a/h = 240) with immovable inplane edges at P_o = 0, 0.1 and 0.2.

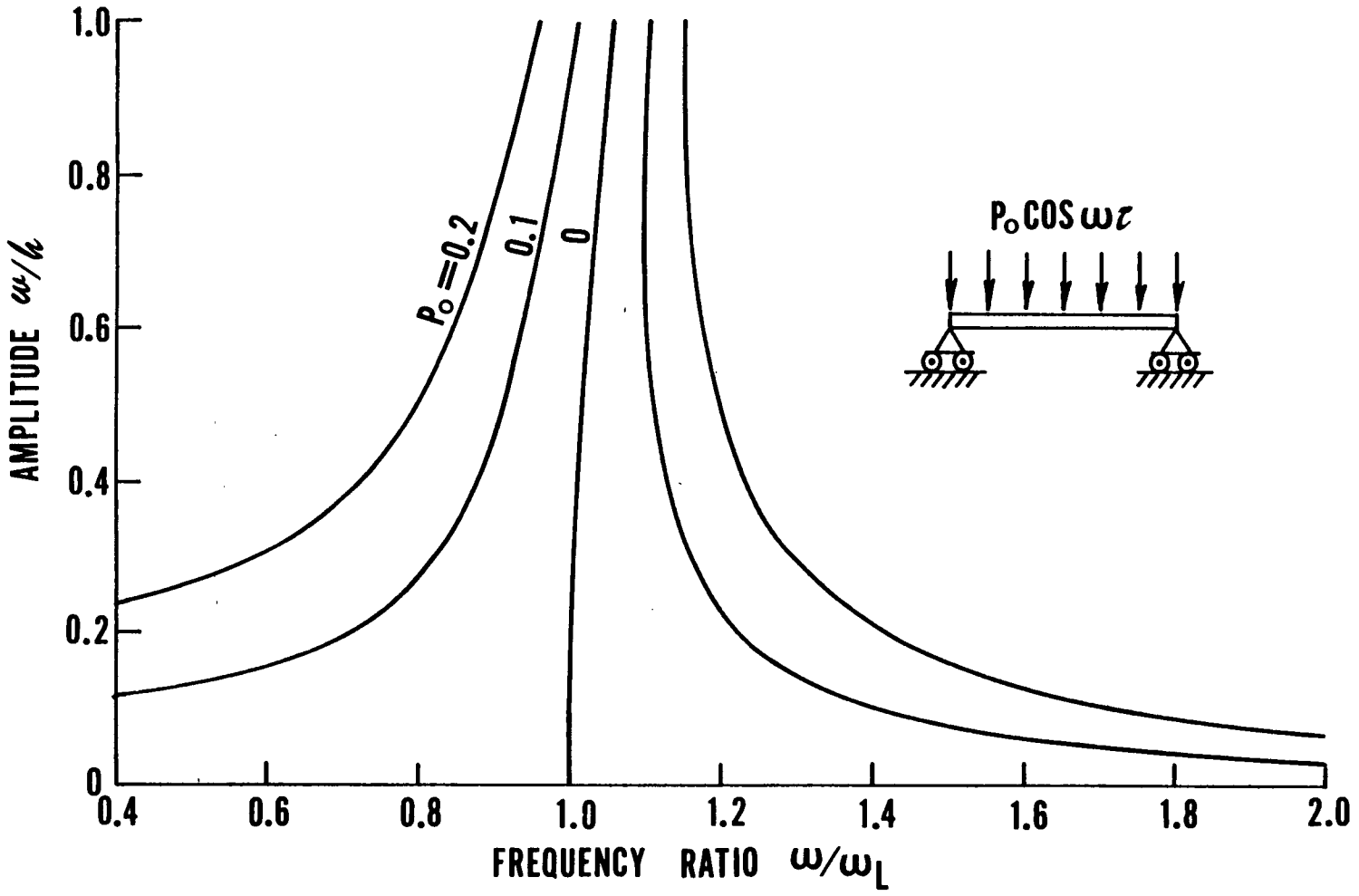

Figure 11. Amplitude versus frequency for a simply supported square plate (a/h = 240) with movable inplane edges at P_o = 0, 0.1 and 0.2.

tude of the concentrated force is equal to the same plate under a uniformly distributed harmonic loading of $P_o = 0.1$ ($F_o = 45.74$ N/m^2 or 0.66347×10^{-2} psi) over the total plate area. Therefore, the uniform loading of the loaded element for the concentrated case is $F_o = 45.74\ (a/d)^2$ N/m^2 where d is the length of the loaded square element. Table VIII gives the fundamental frequency ratios ω/ω_L at $(d/a)^2 = 16.0$, 4.0, 1.0 and 0.25%. It indicates that the convergence is rapid and $(d/a)^2 = 1.0\%$ would yield accurate frequency response. Results obtained using earlier finite element without IDI and elliptic function (with in plane deformation but no inplane inertia) are also given. Nonlinear response of concentrated force obtained with $(d/a)^2 = 1.0\%$ is plotted in figure 12. Frequency ratios of the same plate to uniform harmonic force $P_o = 0.2$ is also given. It shows that the concentrated force is approximately two to three times as much severe as the uniformly distributed force for the case studied.

CONCLUSIONS

The finite element method has been extended to analyze nonlinear forced vibration problems. Harmonic force matrices were developed for a beam and a rectangular plate element subjected to uniform harmonic excitation. Improved finite element results on nonlinear free flexural vibration of slender beams and thin plates are achieved by considering inplane deformation and inertia effects in the formulation. Nonlinear free vibration can be simply treated as a limiting case of the more general forced vibration problem by setting the harmonic force matrix equal to zero. The effect of midplane stretching due to large deflection is to increase the nonlinearity, however, the effects of inplane deformation and inertia are to reduce nonlinearity.

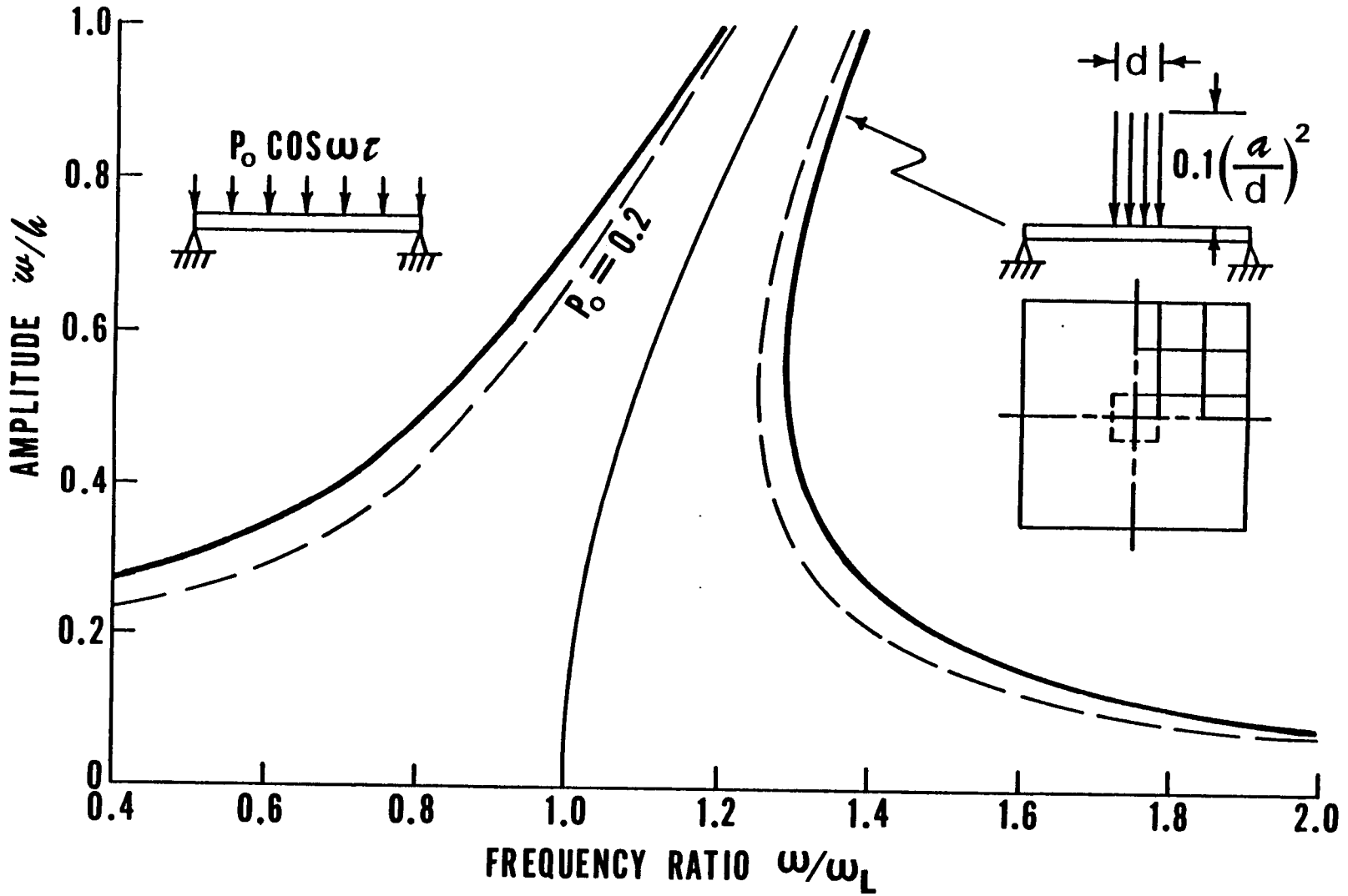

Figure 12. Amplitude versus frequency for a simply supported square plate (a/h = 240) with immovable inplane edges under concentrated loading.

For beams with immovable end supports, only hardening type nonlinearity is observed. For beams of large slenderness ratio with a movable axial end support, the increase in nonlinearity due to large deflection is partially compensated by the reduction in nonlinearity due to longitudinal deformation and inertia. This leads to a negligible hardening type nonlinearity, and thus small deflection linear solution can be used, i.e. a simply supported beam with movable axial end support. For beams of small slenderness ratio, however, softening type nonlinearity is observed.

For rectangular plates with immovable or movable inplane edges, however, only hardening type nonlinearity is observed. This is because the middle surface of the bent plate is not a developable surface.

For concentrated loading (beams and rectangular plates) yields responses several times as severe as the uniformly distributed load. Fatigue life can be estimated with material fatigue S-N data.

APPENDIX A: BEAM ELEMENT

The nonlinear strain-displacement relation is

$$\varepsilon = e + z\,\kappa$$

$$= \frac{\partial u}{\partial x} + \frac{1}{2}\left(\frac{\partial w}{\partial x}\right)^2 - z\,\frac{\partial^2 w}{\partial x^2} \qquad \text{(A1)}$$

Axial resultant force and bending moment are given by

$$N = ESe$$

$$= ES\left[\frac{\partial u}{\partial x} + \frac{1}{2}\left(\frac{\partial w}{\partial x}\right)^2\right] \qquad \text{(A2)}$$

$$M = EI\,\kappa$$

$$= -EI\,\frac{\partial^2 w}{\partial x^2} \qquad \text{(A3)}$$

The bending strain, membrane strain and kinetic energies are

$$U_b = \frac{EI}{2}\int_0^{\ell}\left(\frac{\partial^2 w}{\partial x^2}\right)^2 dx \qquad \text{(A4)}$$

$$U_m = \frac{ES}{2}\int_0^{\ell}\left[\frac{\partial u}{\partial x} + \frac{1}{2}\left(\frac{\partial w}{\partial x}\right)^2\right]^2 dx \qquad \text{(A5)}$$

$$T = \frac{\rho S}{2} \int_0^{\ell} (\dot{u}^2 + \dot{w}^2)\, dx \tag{A6}$$

where ℓ and S are the length and cross-sectional area of the beam element. The displacement function is chosen as

$$w = \alpha_1 + \alpha_2 x + \alpha_3 x^2 + \alpha_4 x^3 \tag{A7}$$

$$u = \beta_1 + \beta_2 x \tag{A8}$$

The element nodal displacements at the two end nodes are

$$\{\delta\}^T = [\{\delta_b\}^T \ \{\delta_m\}^T]$$

$$= [W_1, \ W_{x1}, \ W_2, \ W_{x2}, \ U_1, \ U_2] \tag{A9}$$

The matrices relate the element nodal displacements and the generalized coordinates are

$$[T_b] = \begin{bmatrix} 1 & 0 & 0 & 0 \\ 0 & 1 & 0 & 0 \\ -\frac{3}{\ell^2} & -\frac{2}{\ell} & \frac{3}{\ell^2} & -\frac{1}{\ell} \\ \frac{2}{\ell^3} & \frac{1}{\ell^2} & -\frac{2}{\ell^3} & \frac{1}{\ell^2} \end{bmatrix} \tag{A10}$$

$$[T_m] = \begin{bmatrix} 1 & 0 \\ -\frac{1}{\ell} & \frac{1}{\ell} \end{bmatrix} \tag{A11}$$

The linearizing function is evaluated from the expression

$$f = \frac{1}{2} \frac{\partial w}{\partial x}$$

$$= \frac{1}{2} [Q]\{\alpha\}$$

$$= \frac{1}{2} \begin{bmatrix} 0 & 1 & 2x & 3x^2 \end{bmatrix} [T_b]\{\delta_b\} \tag{A12}$$

The matrix relates generalized coordinates and membrane strain defined in equation (26) is

$$[G] = [0 \quad 1] \tag{A13}$$

The element harmonic force matrix is

$$[p] = \frac{cF_o\ell}{420AR} \begin{bmatrix} 156 & & & \text{symmetric} \\ 22\ell & 4\ell^2 & & \\ 54 & 13\ell & 156 & \\ -13\ell & -3\ell^2 & -22\ell & 4\ell^2 \end{bmatrix} \tag{A14}$$

The total strains at the two end nodes of a beam element are

$$\begin{Bmatrix} \varepsilon_1 \\ \varepsilon_2 \end{Bmatrix} = \begin{bmatrix} 0 & f & -2z & 0 & 0 & 1 \\ 0 & f & 2(\ell f - z) & 3(\ell^2 f - 2\ell z) & 0 & 1 \end{bmatrix} \begin{bmatrix} T_b & 0 \\ 0 & T_m \end{bmatrix} \{\delta\} \tag{A15}$$

APPENDIX B: PLATE ELEMENT

The inverse of matrix $[T_b]$ in equation (21) is given by

$$[T_b]^{-1} = \begin{array}{c} \begin{matrix} \alpha_1 & & & \alpha_4 & & & & \alpha_8 & & & & \alpha_{12} & & & & \alpha_{16} \end{matrix} \\ \begin{bmatrix} 1 & 0 & 0 & 0 & 0 & 0 & 0 & 0 & 0 & 0 & 0 & 0 & 0 & 0 & 0 & 0 \\ 1 & \bar{a} & 0 & \bar{a}^2 & 0 & 0 & \bar{a}^3 & 0 & 0 & 0 & 0 & 0 & 0 & 0 & 0 & 0 \\ 1 & \bar{a} & \bar{b} & \bar{a}^2 & \bar{a}\bar{b} & \bar{b}^2 & \bar{a}^3 & \bar{a}^2\bar{b} & \bar{a}\bar{b}^2 & \bar{b}^3 & \bar{a}^3\bar{b} & \bar{a}^2\bar{b}^2 & \bar{a}\bar{b}^3 & \bar{a}^3\bar{b}^2 & \bar{a}^2\bar{b}^3 & \bar{a}^3\bar{b}^3 \\ 1 & 0 & \bar{b} & 0 & 0 & \bar{b}^2 & 0 & 0 & 0 & \bar{b}^3 & 0 & 0 & 0 & 0 & 0 & 0 \\ 0 & 1 & 0 & 0 & 0 & 0 & 0 & 0 & 0 & 0 & 0 & 0 & 0 & 0 & 0 & 0 \\ 0 & 1 & 0 & 2\bar{a} & 0 & 0 & 3\bar{a}^2 & 0 & 0 & 0 & 0 & 0 & 0 & 0 & 0 & 0 \\ 0 & 1 & 0 & 2\bar{a} & \bar{b} & 0 & 3\bar{a}^2 & 2\bar{a}\bar{b} & \bar{b}^2 & 0 & 3\bar{a}^2\bar{b} & 2\bar{a}\bar{b}^2 & \bar{b}^3 & 3\bar{a}^2\bar{b}^2 & 2\bar{a}\bar{b}^3 & 3\bar{a}^2\bar{b}^3 \\ 0 & 1 & 0 & 0 & \bar{b} & 0 & 0 & 0 & \bar{b}^2 & 0 & 0 & 0 & \bar{b}^3 & 0 & 0 & 0 \\ 0 & 0 & 1 & 0 & 0 & 0 & 0 & 0 & 0 & 0 & 0 & 0 & 0 & 0 & 0 & 0 \\ 0 & 0 & 1 & 0 & \bar{a} & 0 & 0 & \bar{a}^2 & 0 & 0 & \bar{a}^3 & 0 & 0 & 0 & 0 & 0 \\ 0 & 0 & 1 & 0 & \bar{a} & 2\bar{b} & 0 & \bar{a}^2 & 2\bar{a}\bar{b} & 3\bar{b}^2 & \bar{a}^3 & 2\bar{a}^2\bar{b} & 3\bar{a}\bar{b}^2 & 2\bar{a}^3\bar{b} & 3\bar{a}^2\bar{b}^2 & 3\bar{a}^3\bar{b}^2 \\ 0 & 0 & 1 & 0 & 0 & 2\bar{b} & 0 & 0 & 0 & 3\bar{b}^2 & 0 & 0 & 0 & 0 & 0 & 0 \\ 0 & 0 & 0 & 0 & 1 & 0 & 0 & 0 & 0 & 0 & 0 & 0 & 0 & 0 & 0 & 0 \\ 0 & 0 & 0 & 0 & 1 & 0 & 0 & 2\bar{a} & 0 & 0 & 3\bar{a}^2 & 0 & 0 & 0 & 0 & 0 \\ 0 & 0 & 0 & 0 & 1 & 0 & 0 & 2\bar{a} & 2\bar{b} & 0 & 3\bar{a}^2 & 4\bar{a}\bar{b} & 3\bar{b}^2 & 6\bar{a}^2\bar{b} & 6\bar{a}\bar{b}^2 & 9\bar{a}^2\bar{b}^2 \\ 0 & 0 & 0 & 0 & 1 & 0 & 0 & 0 & 2\bar{b} & 0 & 0 & 0 & 3\bar{b}^2 & 0 & 0 & 0 \end{bmatrix} \end{array} \tag{B1}$$

where $\bar{a}$ and $\bar{b}$ are the length and width of rectangular plate element.

Matrix $[T_m]$ in equation (22) is given by

$$[T_m] = \begin{bmatrix} U_1 & & & U_4 & V_1 & & & V_4 \\ 1 & 0 & 0 & 0 & & & & \\ -a^* & a^* & 0 & 0 & & & & \\ -b^* & 0 & 0 & b^* & & 0 & & \\ a^*b^* & -a^*b^* & a^*b^* & -a^*b^* & & & & \\ & & & & 1 & 0 & 0 & 0 \\ & & & & -a^* & a^* & 0 & 0 \\ & 0 & & & -b^* & 0 & 0 & b^* \\ & & & & a^*b^* & -a^*b^* & a^*b^* & -a^*b^* \end{bmatrix} \quad \text{(B2)}$$

where $a^* = 1/\overline{a}$ and $b^* = 1/\overline{b}$.

Matrix [H] in equation (23) is of the form

$$[H] = -\begin{bmatrix} \alpha_1 & & & \alpha_4 & & & \alpha_8 & & & & \alpha_{12} & & & & & \alpha_{16} \\ 0 & 0 & 0 & 2 & 0 & 0 & 6x & 2y & 0 & 0 & 6xy & 2y^2 & 0 & 6xy^2 & 2y^3 & 6xy^3 \\ 0 & 0 & 0 & 0 & 0 & 2 & 0 & 0 & 2x & 6y & 0 & 2x^2 & 6xy & 2x^3 & 6xy^2 & 6x^3y \\ 0 & 0 & 0 & 0 & 2 & 0 & 0 & 4x & 4y & 0 & 6x^2 & 8xy & 6y^2 & 12x^2y & 12xy^2 & 18x^2y^2 \end{bmatrix}$$

(B3)

Matrix [Q] in equation (25) is

$$[Q] = \begin{bmatrix} \alpha_1 & & & \alpha_4 & & & \alpha_8 & & & & \alpha_{12} & & & & & \alpha_{16} \\ 0 & 1 & 0 & 2x & y & 0 & 3x^2 & 2xy & y^2 & 0 & 3x^2y & 2xy^2 & y^3 & 3x^2y^2 & 2xy^3 & 3x^2y^3 \\ 0 & 0 & 1 & 0 & x & 2y & 0 & x^2 & 2xy & 3y^2 & x^3 & 2x^2y & 3xy^2 & 2x^3y & 3x^2y^2 & 3x^3y^2 \end{bmatrix}$$

(B4)

Matrix [G] in equation (26) is given by

$$[G] = \begin{matrix} \\ \\ \\ \end{matrix} \begin{matrix} \beta_1 & & & \beta_4 & & & & \beta_8 \end{matrix} \begin{bmatrix} 0 & 1 & 0 & y & 0 & 0 & 0 & 0 \\ 0 & 0 & 0 & 0 & 0 & 0 & 1 & X \\ 0 & 0 & 1 & X & 0 & 1 & 0 & y \end{bmatrix} \qquad (B5)$$

REFERENCES

1. Woinowsky-Krieger, S.: The Effect of an Axial Force on the Vibrations of Hinged Bars. J. Appl. Mech., Vol. 17, 1950, pp. 35-36.

2. Herrmann, G.: Influence of Large Amplitude on Flexural Motion of Elastic Plates, NACA TN 3578, 1956.

3. Chu, H.N. and Herrmann, G.: Influence of Large Amplitudes on Free Flexural Vibrations of Rectangular Elastic Plates. J. Appl. Mech., Vol. 23, 1956, pp. 532-540.

4. Eisley, J.G.: Nonlinear Vibration of Beams and Rectangular Plates. Zeitschrift fur angewandte Mathematik and Physik, Vol. 15, 1964, pp. 167-175.

5. Srinivasan, A.V.: Nonlinear Vibrations of Beams and Plates, Int. J. Non-Linear Mechanics, Vol. 1, 1966, pp. 179-191.

6. Bennett, J.A. and Eisley, J.G.: A Multiple Degree-of-Freedom Approach to Non-linear Beam Vibrations. AIAA J., Vol. 8, 1970, pp. 743-749.

7. Eisley, J.G. and Bennett, J.A.: Stability of Large Amplitude Forced Motion of a Simply Supported Beam. Int. J. Non-Linear Mechanics, Vol. 5, 1970, pp. 645-657.

8. Busby, H.R. and Weingarten, V.I.: Non-linear Response of a Beam to Periodic Loading. Int. J. Non-Linear Mechanics, Vol. 7, 1972, pp. 289-303.

9. Lou, C.L. and Sikarskie, D.L.: Non-linear Vibrations of Beam Using a Form-Function Approximation. J. Appl. Mech., Vol. 42, 1975, pp. 209-214.

10. Cheung, Y.K. and Lau, S.L.: Incremental Time-Space Finite Strip Method for Non-linear Structure Vibrations. Earthquake Engineering and Structural Dynamics, Vol. 10, 1982, pp. 239-253.

11. Nayfeh, A.G., Mook, D.T., and Sridhar, S.: Nonlinear Analysis of the Forced Response of Structural Elements. J. Acoustical Soc. America, Vol. 55, 1974, pp. 281-291.

12. Nayfeh, A.H., Mook, D.T., and Lobitz, D.W.: A Numerical-Perturbation Method for the Non-linear Analysis of Structural Vibrations. AIAA J., Vol. 12, 1974, pp. 1222-1228.

13. Eisley, J.G.: Nonlinear Deformation of Elastic Beams, Rings and Strings. Appl. Mech. Review, Vol. 16, 1963, pp. 677-680.

14. Sathyamoorthy, M.: Nonlinear Analysis of Beams Part I: A Survey of Recent Advances. Shock and Vib. Digest, Vol. 14, 1982, pp. 19-35.

15. Yamaki, N.: Influence of Large Amplitudes on Flexural Vibrations of Elastic Plates. Zeitschrift fur angewandte Mathematik and Mechanik, Vol. 41, 1961, pp. 501-510.

16. Lin, Y. K.: Response of a Nonlinear Flat Panel to Periodic and Randomly-Varying Loadings. J. Aerospace Science, Vol. 29, 1962, pp. 1029-1034, 1066.

17. Kung, G.C., and Pao, Y.H.: Nonlinear Flexural Vibrations of a Clamped Circular Plate. J. Applied Mechanics, Vol. E-39, 1972, pp. 1050-1054.

18. Yamaki, N., Otomo, K. and Chiba, M.: Nonlinear Vibrations of a Clamped Circular Plate with Initial Deflection and Initial Edge Displacement, Part 1: Theory. J. Sound and Vibration, Vol. 79, 1981, pp. 23-42.

19. Huang, C.L. and Sandman, B.E.: Large Amplitude Vibrations of a Rigidly Clamped Circular Plates. Int. J. Non-Linear Mechanics, Vol. 6, 1971, pp. 451-468.

20. Huang, C.L. and Al-khattat.: Finite Amplitude Vibrations of a Circular Plate. Int. J. Non-linear Mechanics, Vol. 12, 1977, pp. 297-306.

21. Rehfield, L.W.: Large Amplitude Forced Vibrations of Elastic Structures. AIAA J., Vol. 12, 1974, pp. 388-390.

22. Sridhar, S., Mook, D.T. and Nayfeh, A.H.: Non-linear Resonances in the Forced Responses of Plates, Part I: Symmetric Responses of Circular Plates. J. Sound and Vibration, Vol. 41, 1975, pp. 359-373.

23. Lobitz, D.W., Nayfeh, A.H. and Mook, D.T.: Non-linear Analysis of Vibrations of Irregular Plates. J. Sound and Vibration, Vol. 50, 1977, pp. 203-217.

24. Sridhar, S., Mook, D.T. and Nayfeh, A.H.: Non-linear Resonances in the Forced Responses of Plates, Part II: Asymmetric Responses in Circular Plates. J. Sound and Vibration, Vol. 59, 1978, pp. 159-170.

25. Lau, S.L., Cheng, Y.K. and Wu, S.Y.: Amplitude Incremental Finite Element for Nonlinear Vibration of Thin Plate. Proc. International Conference on Finite Element Methods, Guangquian, H. and Cheung, Y.K., eds., 1982, pp. 184-190.

26. Berger, H.M.: A New Approach to the Analysis of Large Deflections of Plates. J. Applied Mechanics, Vol. 22, 1955, pp. 465-472.

27. Wah, T.: Large Amplitude Flexural Vibration of Rectangular Plates. Int. J. Mech., Sci., Vol. 5, 1963, pp. 3-16.

28. Ramachandran, J.: Non-linear Vibrations of Circular Plates with Linearly Varying Thickness. J. Sound and Vibration, Vol. 38, 1975, pp. 225-232.

29. Chia, C.Y.: Nonlinear Analysis of Plates, McGraw-Hill, 1980.

30. Sathyamoorthy, M.: Nonlinear Vibrations of Plates - A Review, Shock and Vibration Digest, Vol. 15, 1983, pp. 3-16.

31. Mei, C.: Nonlinear Vibration of Beams by Matrix Displacement Method. AIAA J., Vol. 10, 1972, pp. 355-357.

32. Mei, C.: Finite Element Displacement Method for Large Amplitude Free Flexural Vibrations of Beams and Plates. Comp. Struc., Vol. 3, 1973, pp. 163-174.

33. Evensen, D.A.,: Nonlinear Vibrations of Beams with Various Boundary Conditions, AIAA J., Vol. 6, 1968, pp. 370-372.

34. Rao, G.V., Raju, I.S. and Raju, K.K.: Finite Element Formulation for the Large Amplitude Free Vibrations of Beams and Orthotropic Circular Plates. Comp. Struc., Vol. 6, 1976, pp. 169-172.

35. Rao, G.V., Raju, I.S., and Raju, K.K.: A Finite Element Formulation for Large Amplitude Flexural Vibrations of Thin Rectangular Plates. Comp. Struc., Vol. 6, 1976, pp. 163-167.

36. Raju, K.K. and Rao, G.V.: Nonlinear Vibrations of Orthotropic Plates by a Finite Element Method. J. Sound Vib., Vol. 48, 1976, pp. 301-303.

37. Rao, G.V., Raju, I.S., and Raju, K.K.: Nonlinear Vibrations of Beams Considering Shear Deformation and Rotary Inertia. AIAA J., Vol. 14, 1976, pp. 685-687.

38. Raju, K.K. and Rao, G.V.: Axisymmetric Vibrations of Circular Plates Including the Effects of Geometric Non-Linearity, Shear Deformation and Rotary Inertia. J. Sound Vib., Vol. 47, 1976, pp. 179-184.

39. Reddy, J.N. and Stricklin, J.D.: Large Deflection and Large Amplitude Free Vibrations of Thin Rectangular Plates Using Mixed Isoparametric Elements. Symposium on Applications of Computer Methods in Engineering, Univ. California, Los Angeles, August 23-26, 1977.

40. Mei, C. and Rogers, J.L., Jr.: Application of the TRPLT1 Element to Large Amplitude Free Vibrations of Plates. NASA CP-2018, 1977, pp. 275-298.

41. Narayanaswami, R. and Mei, C.: Addition of Higher-Order Plate Elements to NASTRAN. NASA TM X-3428, 1976, pp. 439-477.

42. Mei, C., Narayanaswami, R., and Rao, G.V.: Large Amplitude Free Flexural Vibrations of Plates of Arbitrary Shape. Comp. Struc., Vol. 10, 1979, pp. 675-681.

43. Cowper, G.R., Kosko, E., Lindberg, G.M., and Olson, M.D.: Static and Dynamic Applications of a High-Precision Triangular Bending Element. AIAA J., Vol. 7, 1969, 1957-1965.

44. Reddy, J.N. and Chao, W.C.: Large-Deflection and Large-Amplitude Free Vibrations of Laminated Composite-Material Plates. Comp. Struc., Vol. 13, 1981, pp. 341-347.